Executive Summary

On August 30, 1999, the South Florida Water Management District (District) contracted with DB Environmental Laboratories, Inc. (DBEL) to perform a 100 week evaluation of Submerged Aquatic Vegetation/Limerock (SAV/LR) Treatment System technology for reducing phosphorus (P) discharge from Everglades Agricultural Area (EAA) waters. The objectives of this project are to assess the long-term, sustainable performance of this technology, and to develop design and operational criteria for a full-scale SAV/LR system. For this effort, we are performing scientific and engineering work at Stormwater Treatment Area (STA)-1W at several spatial scales: outdoor microcosms and mesocosms, test cells (0.2 ha), Cell 4 (146 ha) and Cell 5 (1,100 ha). This document is a quarterly progress report describing work efforts of DBEL's project team from September 1999-January 2000. Key accomplishments and findings are as follows.

During this quarter, we continued using existing mesocosms at both the North and South Supplemental Technology sites of STA-1W to assess effects of hydraulic loading rates, water type (Post-BMP vs. Post-STA), and system configuration on SAV/LR P removal performance.

In preparation for changing the "Static Water Depth" experiment to a "Fluctuating Water Depth" experiment, we performed P mass balances on SAV mesocosms that had been operated at three separate water depths (0.4, 0.8 and 1.2m) for 15.5 months. Of the calculated mass of P removed based on mesocosm inflow – outflow measurements, we recovered between 58 – 86% of this P in the plant standing crop and sediments. Average sediment P storage, the long-term P sink in SAV wetlands, ranged from 0.84 to 2.02 gP/m^2-yr.

We performed spatial and temporal water quality sampling in two mesocosm experiments (Static Water Depth and Sequential SAV/LR) to better define P removal mechanisms in SAV systems. In the Static Water Depth mesocosms, which were providing good P removal performance, we observed a close correlation between daytime pH, soluble reactive P (SRP) removal and calcium (Ca) removal. In the Sequential Systems, which were not removing P well due to partial mortality of the *Chara* standing crop, the correlations among SRP removal, Ca removal and pH were poor.

We continued long-term monitoring of SAV/LR mesocosms that receive Post-BMP waters at three separate hydraulic loading rates (HLRs) of 11, 22 and 55 cm/day. Effluent TP concentrations over a 19 month period (June 1998 through January 2000) for these respective HLR treatments have averaged 18, 23 and 45 µg/L.

We continued long-term monitoring of shallow (0.09 m deep) SAV/periphyton/LR raceways that receive Post-STA waters. Influent, raceway effluent, and LR effluent TP concentrations over an 18 month period (July 1998 through January 2000) have averaged 18, 10 and 8 µg/L, respectively. In deeper (0.4m) tanks that receive Post-STA waters, we are culturing SAV on muck, sand and limerock substrates. To date, the SAV on the muck substrate appears the most robust, and is providing the lowest effluent TP concentrations (13 µg/L over seven months).

In the 0.2 ha test cells, we performed inflow – outflow monitoring of total P to establish background performance prior to installation of limerock berms. The two northern SAV test cells, operated at a HLR of 10 – 13 cm/day, effectively removed P, providing effluent TP concentrations in the range of 20 – 30 µg/L. By contrast, the two southern SAV test cells provided almost no TP removal. The poor performance of the southern test cells may be due to the more recalcitrant nature of P in the inflow waters at this location, or to the presence of *Hydrilla* as the dominant SAV species. The potential P removal performance of *Hydrilla*, which occurs in Cells 1 and 3 of STA-1W, is unknown. Limerock berm installation for two of the test cells (one north, one south) will begin in March 2000.

Using the test cells, we also performed tracer studies on two dates to further our understanding of the hydraulic characteristics of small wetlands dominated by SAV. Our analyses of the tracer results suggest that the effects of water stage change on hydraulic performance of SAV wetlands can be dramatic. Time-of-travel, short-circuiting, retention time, and wetland dispersion number are hydraulic characteristics that were influenced by the water stage.

STA-1W Cell 5 was flooded in late spring 1999, but has continued to exhibit high water column levels of both phosphorus and color. The previously disturbed (farmed) organic soils are thought to be the source of the high water column constituent concentrations. We tested the effectiveness of lime to improve water quality by deploying *in situ* chambers to isolate small

portions of the Cell 5 sediments and water column. Lime dosages of 66 mg/L and 198 mg/L provided immediate, significant reductions of TP, SRP and true color concentrations. Levels of all constituents began to increase after two to three weeks, however, suggesting that repeated lime applications would be required to maintain long-term P removal.

During this quarter, we collected and reviewed historic Cell 4 performance data and also initiated forecast model development. Cell 4, which is dominated by *Najas* and *Ceratophyllum*, has continued to provide exemplary P removal performance. Using the latest available data (January – June 1999), for example, Cell 4 outflow TP concentrations averaged 13 µg/L. The P mass removal rate during this six month period averaged 1.28 g/m^2-yr.

As a first step in SAV predictive model development, we developed, programmed, and calibrated two lumped-parameter models based on Cell 4 data: a dynamic TP removal model and a parallel-path SRP and (PP+DOP) removal model. Our future efforts will use these programmed models as templates for developing a process-based SAV performance model.

Table of Contents

List of Figures

List of Tables

Introduction

On August 30, 1999, the District contracted with DB Environmental Laboratories, Inc. (DBEL) to design, construct, operate, and evaluate a 100 week, multi-scale demonstration of SAV/ Lime-rock Treatment System technology for reducing phosphorus (P) discharge from Everglades Agricultural Area (EAA) waters. The objectives of this project are to:

- Design and execute a scientific and engineering research plan for further evaluation of the technical, economic and environmental feasibility of using SAV/LR system for P removal at both the basin and sub-basin scale.

- Obtain samples adequate to conduct a Supplemental Technology Standard of Comparison (STSOC) analysis.

- Provide information and experience needed to design a full-scale SAV/LR system.

This document is a quarterly progress report describing work efforts during September 1999-January 2000. This report focuses on methodology and findings from the mesocosm experiments (Task 5), Test Cell studies (Task 6), development of a performance forecast model (Task 9) and Cell 5 inoculation studies (Task 10).

Task 5. Mesocosm Investigations

During September 1999-January 2000, we continued using existing mesocosms at both the North and South Supplemental Technology sites of STA-1W to assess effects of hydraulic loading rates, water type (Post-BMP vs. Post-STA), and system configuration on P removal performance. Activities are listed below by experimental subtask.

Fluctuating Water Depths (Subtask 5ii)

We terminated the Static Depth Study on November 10, 1999 in preparation for initiating the Fluctuating Water Depth investigation (Subtask 5ii), which calls for using the same mesocosm tanks as had been used in Phase I. Two major research efforts were performed prior to and during the "close-out" of the Static Depth mesocosms. These are described below.

Spatial-Temporal Water Column Investigations

The results of our first spatial-temporal diel study in February 1999 for each of the three depth treatments was reported in the Final Report of our Phase I Demonstration Project (DBEL 1999). This study was performed under cool temperature conditions, with only a partially mature plant community. We undertook a second spatial-temporal study on September 24-25, 1999, to document the chemical and physical spatial and temporal variations within the water column with a more mature community and under warmer temperatures.

Water samples were collected and field measurements (pH, D.O., redox potential, and temperature) performed at several depths (3 and 30 cm for shallow mesocosms; 3, 30, and 60 cm for moderate depth mesocosms; and 3, 30, 60, and 90 cm for deep mesocosms) at both the influent (near the splash zone behind the baffle) and effluent regions of the mesocosms. These measurements were performed during both afternoon (1215-1800) and early morning (0200-0645). Water samples were returned to the laboratory and analyzed for the following parameters: calcium (Ca), alkalinity, soluble reactive P (SRP), total soluble P (TSP) and total phosphorus (TP). Total P was measured only on surface samples (3 cm) due to the difficulty of collecting undisturbed

samples at subsurface depths. Alkalinity and Ca analyses were performed on only the shallowest and deepest stations.

Mean characteristics of the afternoon and early morning (pre-dawn) inflow Post-BMP waters during this sampling event were: 84 and 82 µg TP/L; 49 and 42 µg SRP/L; 18 and 19 µg DOP/L; 17 and 17 µg PP/L; 112 and 111 mg Ca/L; and 351 and 293 mg alkalinity (as $CaCO_3$)/L.

Total P concentrations at the influent region of the mesocosms were markedly lower than the TP levels in the inflow waters. (Figure 1). Surface TP concentrations decreased further towards the effluent region of each mesocosm, with minimal concentration differences observed between the afternoon and early morning sampling times within a given depth treatment. There were also minimal effluent TP concentration differences among the three depth treatments (Figure 1).

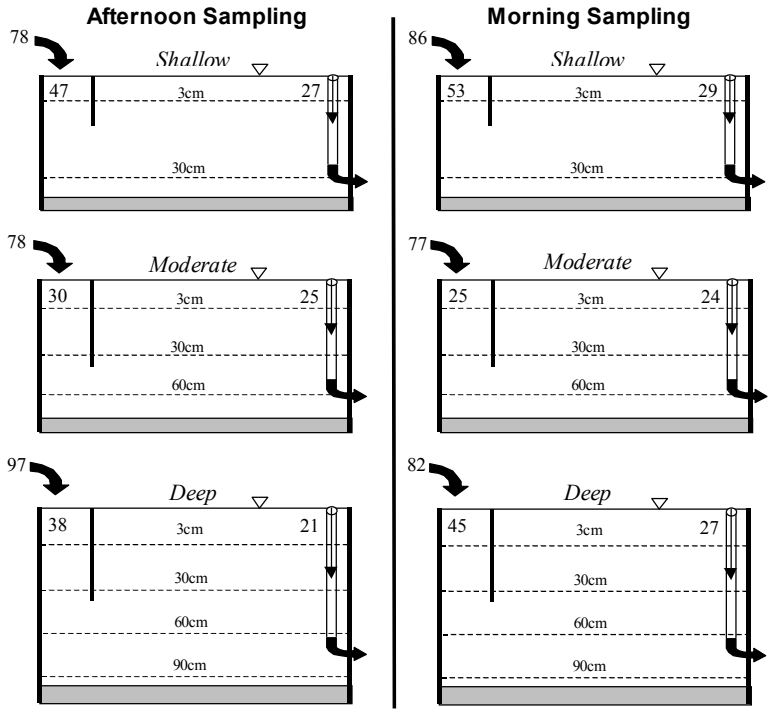

Figure 1. Mean total phosphorus concentration (µg/L) profiles during the Spatial-Temporal study on September 23-24, 1999 in the Static Depth treatments (shallow = 0.4 m, moderate = 0.8 m, deep = 1.2 m) at the North Supplemental Technology Site. Each P concentration within a treatment is a mean of duplicate mesocosms, except for the inflow concentrations.

The labile nature of SRP within SAV systems is readily seen by the large decreases from the inflow SRP concentrations (Figure 2). Even at the influent ends of each mesocosm, SRP concentrations

were considerably lower than inflow levels. Soluble reactive P exhibited more of a dramatic concentration decrease along the horizontal gradient than did total P (cf. Figure 1 and Figure 2). The SRP concentrations at the effluent ends of the mesocosms were near the method detection limit (2 µg/L) in all depth treatments, regardless of the sampling time.

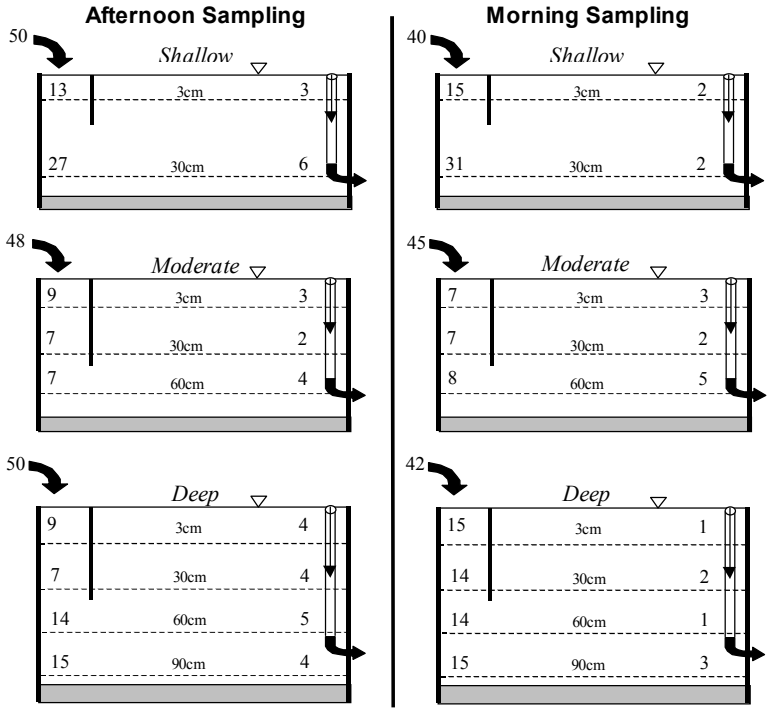

Figure 2. Mean soluble reactive phosphorus concentration (µg/L) profiles during the Spatial-Temporal Study on September 23-24, 1999 in the Static Depth treatments (shallow = 0.4 m, moderate = 0.8 m, deep = 1.2 m). Each SRP concentration within a treatment is a mean of duplicate mesocosms, except for the inflow concentrations.

Figure 3. Mean dissolved oxygen concentration (mg/L) profiles during the Spatial-Temporal Study on September 23-24, 1999 in the Static Depth treatments (shallow = 0.4 m, moderate = 0.8 m, deep = 1.2 m). Each DO concentration within a treatment is a mean of duplicate mesocosms.

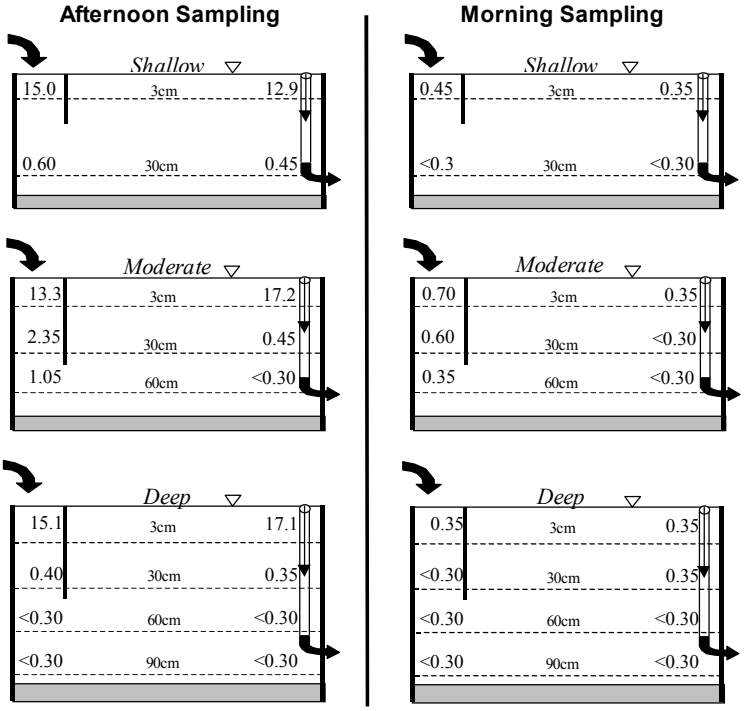

Sediment-water column P fluxes in wetlands are often controlled by iron (Fe). In our mesocosms, the SRP profiles are not what would be expected if the equilibrium P concentrations were dominated by iron chemistry. Dissolved oxygen concentrations were usually below the detection limit of 0.3 mg/L in the 30-90 cm depth zones of all treatments (Figure 3), indicating that the bottom waters and sediments were anoxic. Redox measurements taken 46 days later (November 10, 1999) showed reducing conditions existed at or below the potentials associated with the reduction of Fe^{3+} to Fe^{2+} (E_h of approximately +100 to +150 mV), especially in the bottom waters (Figure 4). Thus if P was bound to oxyhydrides of Fe, an increase in SRP should have been recorded within the mesocosms during the spatial-temporal investigation, particularly during the early morning hours.

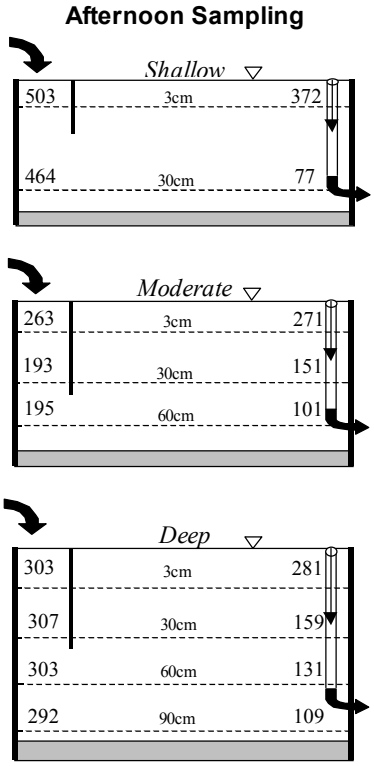

Figure 4. Mean values for daytime E_h (mV) on November 10, 1999 from three replicates of shallow (0.4 m), moderate (0.8 m) and deep (1.2 m) mesocosms of the Static-Depth experiment.

Calcium and alkalinity concentrations within the influent region of the mesocosms were also lower than those of the inflow waters (Figure 5 and Figure 6). However, there was a more marked diel pattern in the spatial Ca and alkalinity concentration changes than was observed for phosphorus.

For example, there were pronounced vertical and horizontal gradients for both parameters in the afternoon, but by early morning they had mostly eroded. Slight horizontal gradients for Ca and alkalinity remained at this time in the shallow and moderate depth mesocosms.

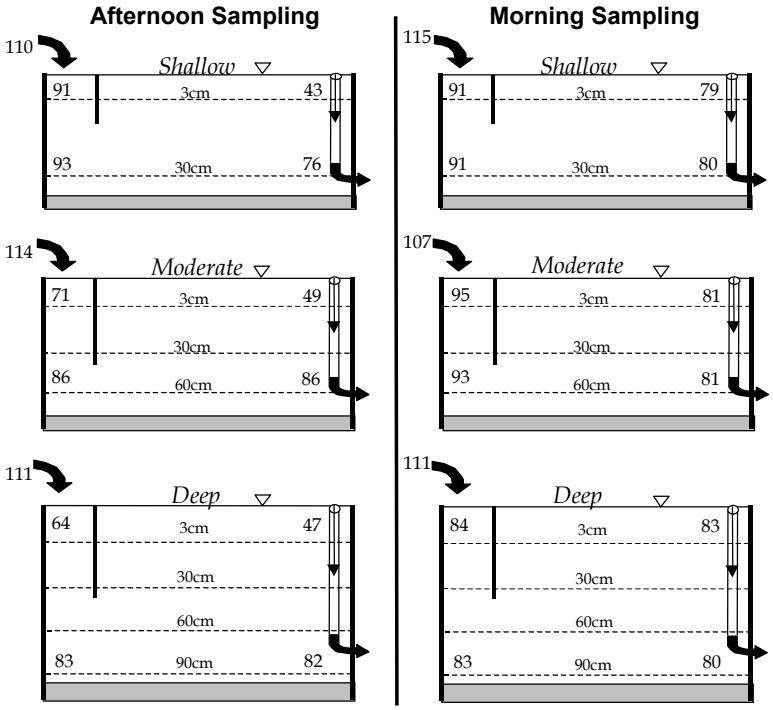

Figure 5. Mean dissolved calcium concentration (mg/L) profiles during the Spatial-Temporal Study on September 23-24, 1999 in the Static Depth treatments (shallow = 0.4 m, moderate = 0.8 m, deep = 1.2 m). Each dissolved Ca concentration within a treatment is a mean of duplicate mesocosms, except for the inflow concentrations.

Figure 6. Mean total alkalinity concentration (mg $CaCO_3$/L) profiles during the Spatial-Temporal Study on September 23-24, 1999 in the Static Depth treatments (shallow = 0.4 m, moderate = 0.8 m, deep = 1.2 m). Each alkalinity concentration within a treatment is a mean of duplicate mesocosms, except for the inflow concentrations.

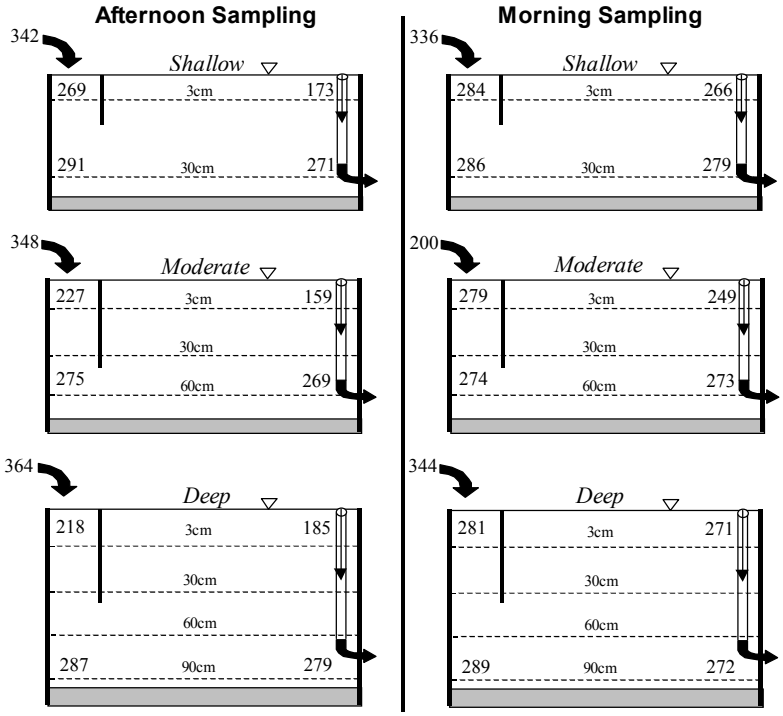

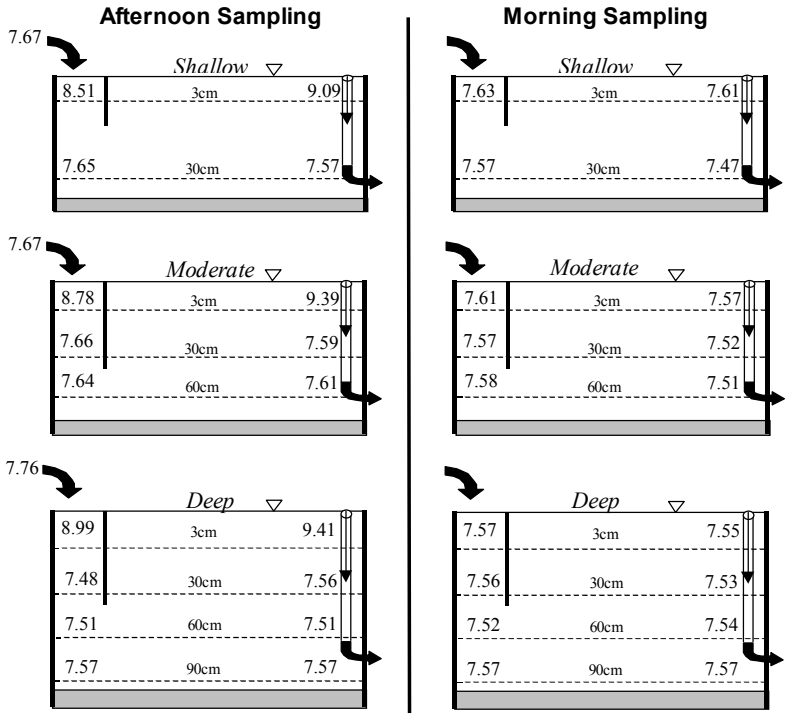

Figure 7. Mean pH value profiles during the Spatial-Temporal Study on September 23-24, 1999 in the Static Depth treatments (shallow = 0.4 m, moderate = 0.8 m, deep = 1.2 m). Each pH value within a treatment is a mean of duplicate mesocosms except for the inflow levels.

The Ca and alkalinity data support the existence of a diel precipitation cycle for calcium carbonate, where pH values increase to above 9.0 in the surface waters during the day (Figure 7), resulting in a supersaturation with respect to calcium carbonate, and ensuing precipitation. In addition to the supersaturation of dissolved carbonate and calcium, the 25-30 $^{\circ}$C water temperatures (Figure 8) would also favor the precipitation of calcium carbonate. Note that the pH values fall to 7.5 - 7.6 during the night, which reduces the saturation index for calcium carbonate precipitation to below 1.0. Under these conditions precipitation is not thermodynamically possible, and this results in the weak horizontal gradient and disappearance of the vertical Ca and alkalinity gradients (Figure 5 and Figure 6).

If P coprecipitation with calcium carbonate is a primary removal mechanism for P in SAV mesocosms, then a relationship between pH, calcium and P would be expected, especially in the surface waters (3 cm depth) during daylight hours. We observed a strong relationship between daytime pH and SRP (r^2 = 0.78) and between Ca and SRP (r^2 = 0.93) for the surface stations, suggesting that P coprecipitation does occur within the euphotic zones of the mesocosms.

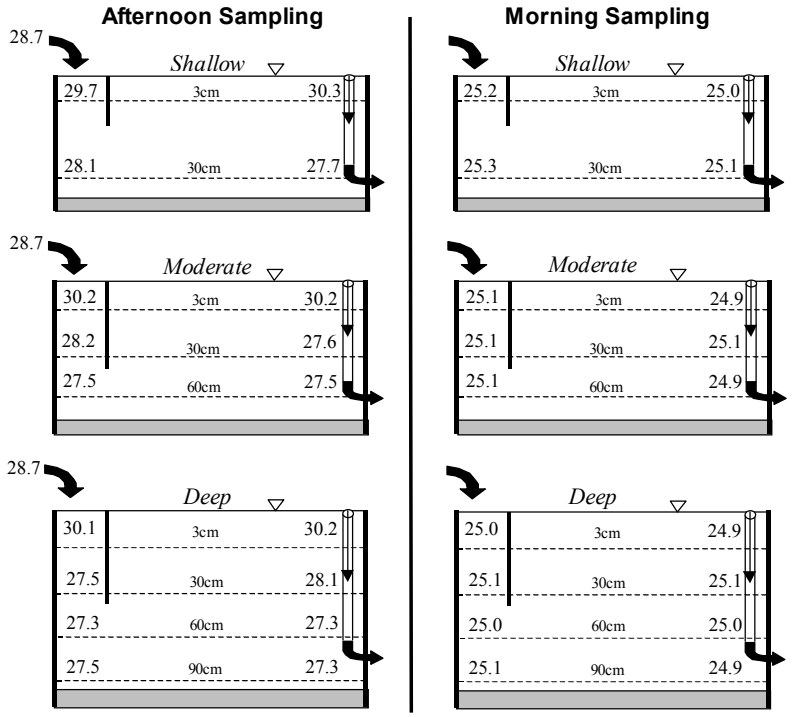

Figure 8. Mean temperature (°C) profiles during the Spatial-Temporal Study on September 23-24, 1999 in the Static Depth treatments (shallow = 0.4 m, moderate = 0.8 m, deep = 1.2 m). Each temperature within a treatment is a mean of duplicate mesocosms, except for the inflow values.

Phosphorus Mass Balances

Upon termination or "close-out" of the Static Depth Study, we sampled the P in vegetation and sediments in order to calculate a P mass balance. During the conduct of this "close-out" mass balance, we minimized physical disturbance to the SAV community by harvesting plants from only 0.76 m^2 (0.38 m^2 quadrats from each of the inflow and outflow regions) within each mesocosm, and retrieving only 10 sediment cores (5 cores [77.5 cm^2] from each of the inflow and outflow regions) from each mesocosm. The harvested SAV biomass was weighed (wet wt), and then returned immediately to the appropriate mesocosms. SAV harvesting was performed on Nov. 10 and 15, 1999; sediments were cored on Nov. 16, 17, and 22. Water quality monitoring was then temporarily discontinued pending re-establishment of the SAV community.

Because of the short duration of the Static Depth experimental period (15.5 months), the accrued sediments were typically only a couple of centimeters thick. The shallow sediment depth, coupled with the dense SAV canopy and roots, made it extremely difficult to accurately sample and measure the accrued sediments within the mesocosms. Although these factors undoubtedly contributed to variability among replicate measurements, we still successfully accounted for most of the P loaded to each mesocosm (Table 1). A higher recovery of P within the mesocosms would likely have been achieved had we harvested the entire plant community and retrieved all the

sediments. As noted above, we instead subsampled those storage compartments because it was necessary to preserve the integrity of the biological community and sediments for the subsequent Fluctuating Water Depth study.

For the Static Depth Study, we observed differences between treatments with respect to the mass of P stored in the SAV biomass and the accrued sediments (Table 1). The P stored in the plant community increased with the depth of the water column. Up to a point, deeper water likely is capable of supporting more SAV biomass than shallower water. The accrued sediment P did not follow the same relationship with water column depth; a greater mass of sediment P was recovered in the shallow depth (0.4 m) mesocosms than in the moderate depth (0.8 m) mesocosms (Table 1).

The relative proportions of the stored P within the SAV and sediment compartments also differed among the water column depth treatments (Table 1). The amount of P stored in the sediments of the shallow depth mesocosms was nearly three times higher than the P mass associated with the SAV. In contrast, 10% and 80% more P was found in the sediments of the moderate and deep mesocosms, respectively, than in their SAV compartments. The differences in the P allocation between the two major storage compartments according to water depth indicates that at least during a "start-up" phase, the shallowest SAV systems are more rapidly storing the removed P in the sediment compartment. Over a longer time period, the sediment is expected to represent the dominant P storage compartment in all SAV systems.

Table 1. Vegetation P storage, P storage in newly deposited sediments, and overall P mass balance for the shallow (SD = 0.4 m), medium (MD = 0.8 m), and deep (DD = 1.2 m) depth mesocosms. Each depth treatment was replicated three times.

Treatment/ Replicate	Phosphorus Mass Removal Rate ($g/m^2 \cdot yr$)				Sediment P to SAV P Ratio	% Recovered
	Input-Output (water)	Storages				
		SAV	Sediment	Total		
SD-1	2.77	0.99	1.71	2.70	1.7	98
SD-2	2.81	0.41	1.32	1.72	3.3	61
SD-3	2.83	0.50	1.46	1.97	3.0	69
SD-Avg.	***2.80***	***0.63***	***1.50***	***2.13***	***2.7***	***76***
MD-1	2.89	0.98	0.87	1.85	0.9	64
MD-2	2.94	0.78	0.83	1.62	1.1	55
MD-3	3.04	0.69	0.83	1.52	1.2	50
MD-Avg.	***2.96***	***0.82***	***0.84***	***1.66***	***1.1***	***58***
DD-1	3.71	0.93	0.99	1.92	1.0	52
DD-2	3.73	1.00	3.34	4.34	3.4	116
DD-3	3.62	1.56	1.76	3.29	1.1	91
DD-Avg.	***3.69***	***1.16***	***2.02***	***3.18***	***1.8***	***86***

Harvesting Effects on Phosphorus Removal (Subtask 5iii)

In a continuing investigation on the effects of plant harvesting, we performed a plant harvest (clipping and discarding the top half of the SAV) on August 19, 1999. A previous harvest was performed during our Phase I study, in September 1998. The P removal efficiency in the mesocosms, which had been considerably reduced after this "second" harvest for a 7-week "recovery" period, returned to near pre-harvest levels by the second week in October (Table 2). We plan to terminate this subtask during the third week of March 2000.

Table 2. Mean influent and effluent total P concentrations (µg/L) of triplicate harvested SAV mesocosms before harvest, and during and after a "recovery" period. Harvesting was performed on August 19, 1999.

	Sampling Events	Influent TP (µg/L)	Effluent TP (µg/L)	P Removal (%)
Pre-Harvest Period (July 1 – Aug 18, 1999)	7	98	29	70
Recovery Period (Aug 19 – Oct 5, 1999)	7	83	84	-1
Post-Recovery Period (Oct 6 – Jan 31, 2000)	13	144	37	74

Long-Term Monitoring (Subtask 5iv)

During November 1999, we established a new sampling schedule for the "long-term monitoring" mesocosms. Biweekly compositing of weekly grab samples for the SAV mesocosm and LR column (both the 1 and 5 hr retention times) influents and effluents was initiated on November 17, 1999. Prior to that, we had collected weekly grabs for SRP and TP and biweekly grabs for TSP, Ca, and alkalinity.

Each of the three "undisturbed" HRT mesocosms (1.5, 3.5, and 7.0 days) remaining from Phase I continued to perform similarly to what had been observed during the Phase I and the "Bridge Funding" (June 1998 to August 1999) periods (Figure 9). That is, effluent SRP and TP concentrations were substantially higher in the 1.5-day HRT mesocosm (12 µg SRP/L and 63 µg TP/L) than in the 3.5- and 7.0-day HRT mesocosms (2 µg SRP/L and 34 µg TP/L for 3.5-day HRT; 2 µg SRP/L and 32 µg TP/L for 7.0-day HRT). The LR columns reduced TP concentrations further in all three respective HRT treatments to 45, 23, and 18 µg/L.

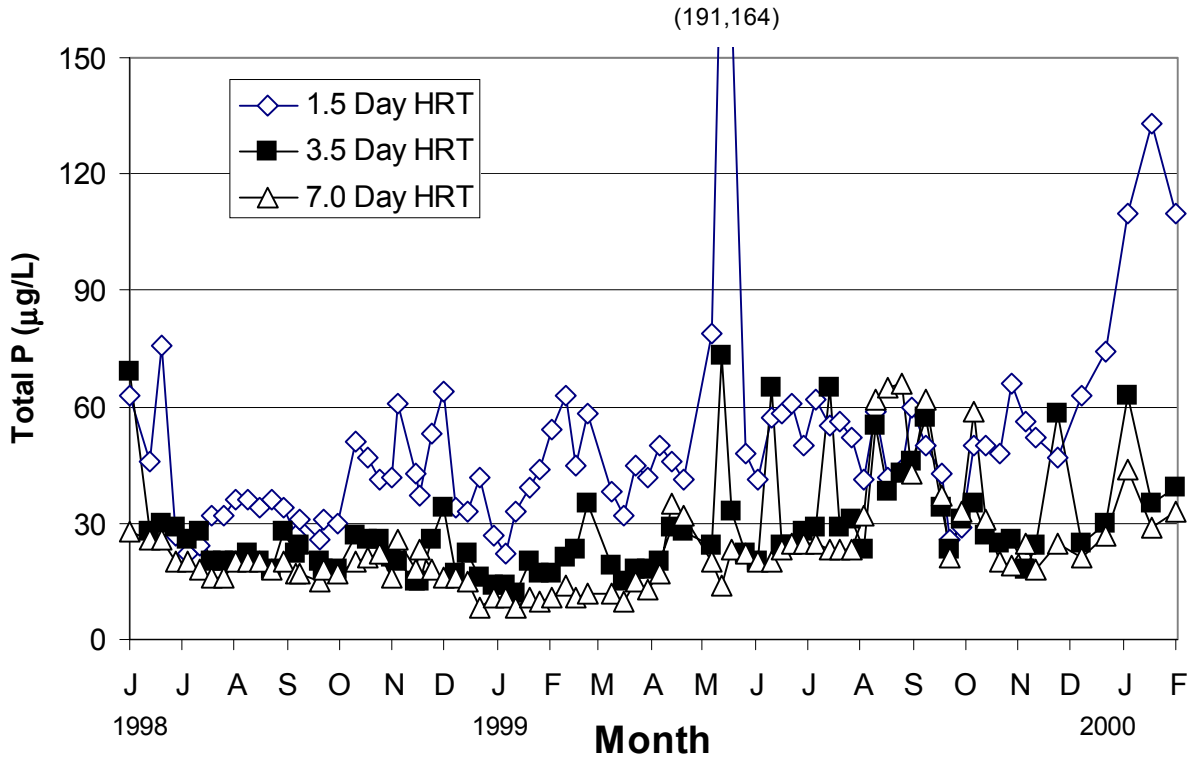

Figure 9. Total phosphorus concentrations in the effluents of undisturbed SAV mesocosms (n=1 for each treatment) operated at 1.5, 3.5 and 7.0 day hydraulic retention times from June 1, 1998 to January 31, 2000.

Pulse Loading and Drydown-Reflooding (Subtask 5v)

On November 17, 1999, we began analyzing two-sample composites of weekly grabs to evaluate background conditions prior to start-up of pulse loading efforts. We had analyzed weekly SRP and TP grabs prior to this time. Sampling for TSP, Ca, and alkalinity was changed from biweekly grabs to biweekly composites on the same date.

Our monitoring data continue to demonstrate that the duplicate mesocosm tanks per HRT treatment intended for deployment in the Pulse Loading and Drydown-Reflooding study in March 2000 have fully recovered from the "sampling disturbance" (SAV harvesting and sediment coring) that was performed in February 1999 (Figure 10). There has been a recent upward trend in effluent concentrations in all treatments, especially in the 1.5-day HRT mesocosms, but this corresponds to a higher TP inflow loading during this period (Figure 11).

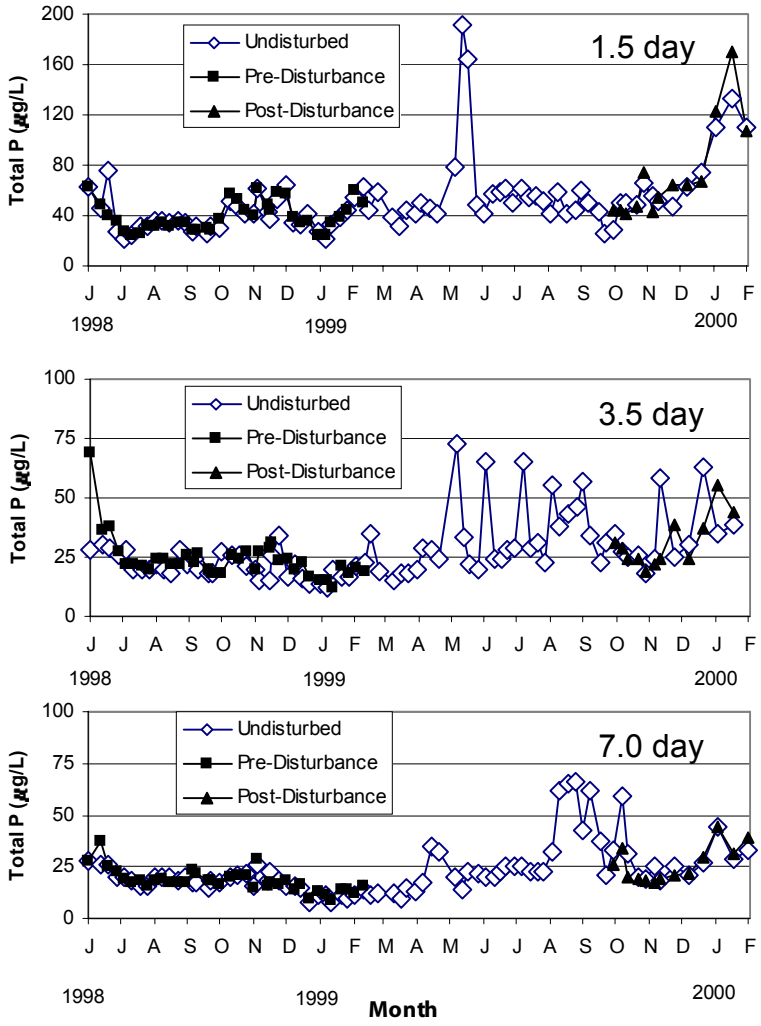

Figure 10. Total P concentrations in undisturbed (no SAV harvesting or sediment coring) and disturbed (SAV harvesting and sediment coring on February 10-11, 1999) mesocosms operated at hydraulic retention times (HRT) of 1.5, 3.5 and 7.0 days. Data from the disturbed mesocosms represent the mean of two replicates and the data from the undisturbed mesocosms are from only one mesocosm per HRT treatment.

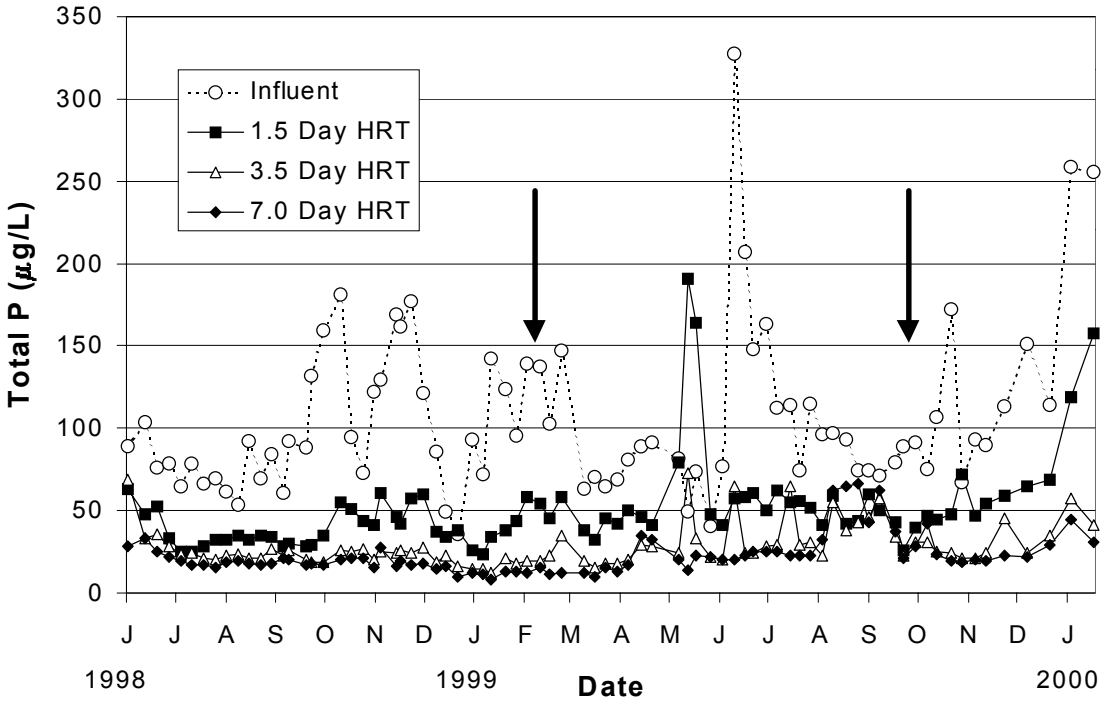

Figure 11. Mean total phosphorus concentrations in the influent and effluents of triplicate mesocosms operated at 1.5, 3.5, and 7.0 day hydraulic retention times (HRT). Data from only one mesocosm of each HRT is presented for the period between February 10 and September 29, 1999 (between arrows).

Sequential SAV/LR Systems and Cattail Mesocosms (Subtask vi)

During our Phase I study, we established a Sequential SAV-LR System that consisted of a deep (0.8 m) mesocosm, a shallow (0.4 m) mesocosm, and a final limerock (LR) bed. Both the deep (0.8 m) and the shallow (0.4 m) SAV mesocosms have undergone considerable shifts in their plant communities since their start-up in June 1998. During the September 1999 to the end of January 2000, deep and shallow mesocosms for the second replicate sequential system were usually devoid of SAV; instead, submersed and surface floating blue-green cyanobacteria mats dominated. The surface floating generae were *Oscillatoria* (8/12/99) and *Lyngbya* (9/21/99) in SAV-2 (deep mesocosm) and a "*Glenodinium*-type" dinoflagellate (8/12/99) in SAV-SD-2 (shallow mesocosm). On the other hand, the SAV in the mesocosms of the first replicate

sequential train persisted, although there were occasional periods when the *Chara* within the shallow mesocosm was stressed to the point of plant mortality and decomposition.

Effluent TP concentrations at all monitoring locations of the Sequential SAV/LR System (i.e., outflows of 0.8 m SAV tanks, 0.4 m SAV tanks, and LR columns) began to increase in May of 1999, peaked during June - August 1999, and (except for the 0.8 m deep mesocosm effluent) have since declined steadily (Figure 12). The long-term mean effluent TP concentrations for the deep and shallow mesocosms and LR barrels corresponded to 63, 25, and 19 µg/L, respectively. We intend to sample the Sequential SAV/LR System until September 2000 to determine whether the observed TP fluctuations follow a seasonal pattern. Additionally, a spatial-temporal water column study was performed during this reporting period, and is described below.

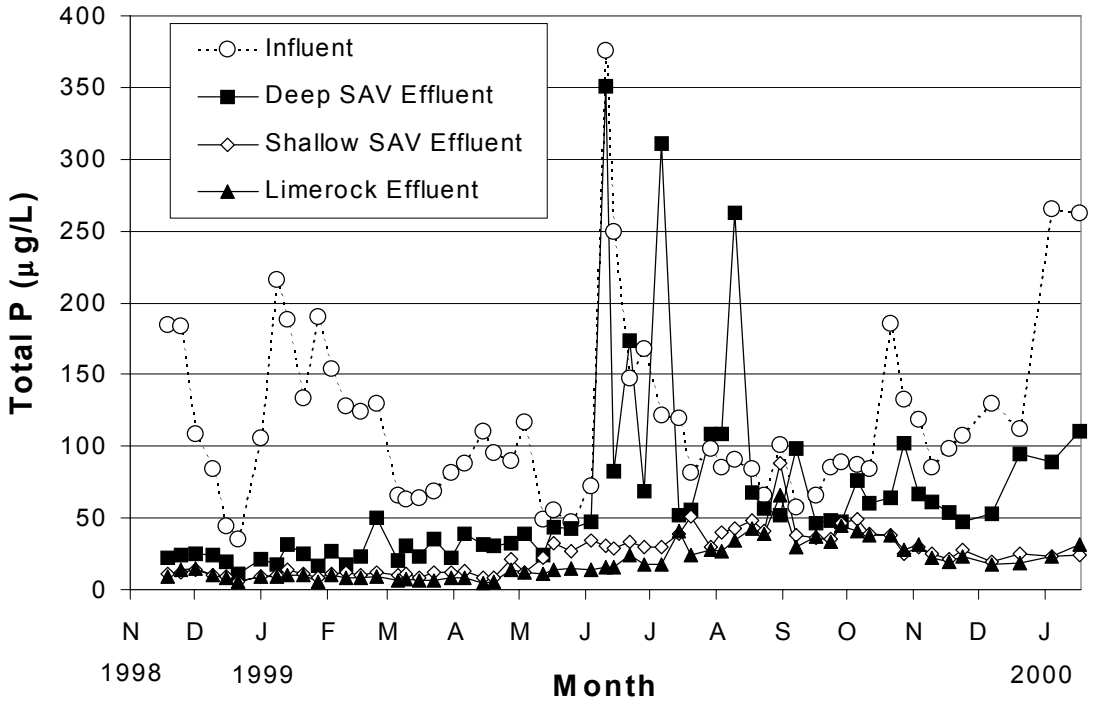

Figure 12. Weekly total P concentrations at four locations in the sequential system treatment train from November 18, 1998 to January 17, 1999. Each effluent value is the mean of duplicate mesocosms and limerock beds.

Spatial-Temporal Water Column Investigation in the Sequential SAV/LR System

In concert with the water column study conducted on the Static Water Depth mesocosms September 23-24, 1999, we also performed similar temporal and spatial sampling in the Sequential SAV/LR mesocosms. The sampling procedures for this effort are described in the Static Water Depth section. Because of the substantial plant community differences between the duplicate sequential treatment mesocosms, the water quality data in Figure 13 - Figure 20 are not averaged values, but instead are reported for each individual mesocosm.

In the initial, deeper mesocosm of the sequential treatment train, replicate 1 was much more efficient in total P removal in both the afternoon and early morning than replicate 2, where no surface horizontal gradient for P was observed. However, the P removal efficiencies were reversed for the two replicate shallow depth "back end" mesocosms: higher P removals were observed in replicate 2 than replicate 1 (Figure 13). For the combined afternoon and morning periods, the final mean effluent total P concentrations leaving the sequential mesocosms was only slightly higher (by 7 µg P/L) in replicate 2 than replicate 1. Even though inflow P concentrations were similar, the

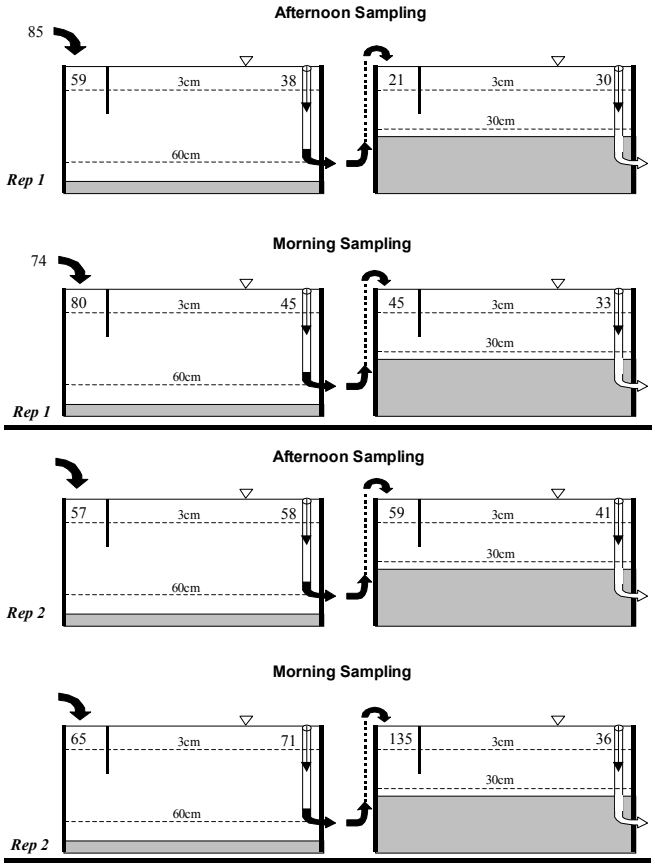

Figure 13. Total phosphorus concentration (µg/L) profiles during the Spatial-Temporal study on September 23-24, 1999 in the Sequential SAV mesocosms at the North Supplemental Technology Site.

sequential mesocosms were less effective at P removal during this time than the static depth mesocosms (cf. Figure 1 and Figure 13).

In both the deep and shallow sequenced tanks, weak vertical SRP concentration profiles existed during both the afternoon and early morning (Figure 14). The horizontal SRP concentration gradients were more pronounced than the vertical concentration gradients, with only a slight diel effect. When compared to the static depth mesocosms sampled at the same times and locations, SRP concentrations within the sequential SAV mesocosms were higher (cf. Figure 2 and Figure 14).

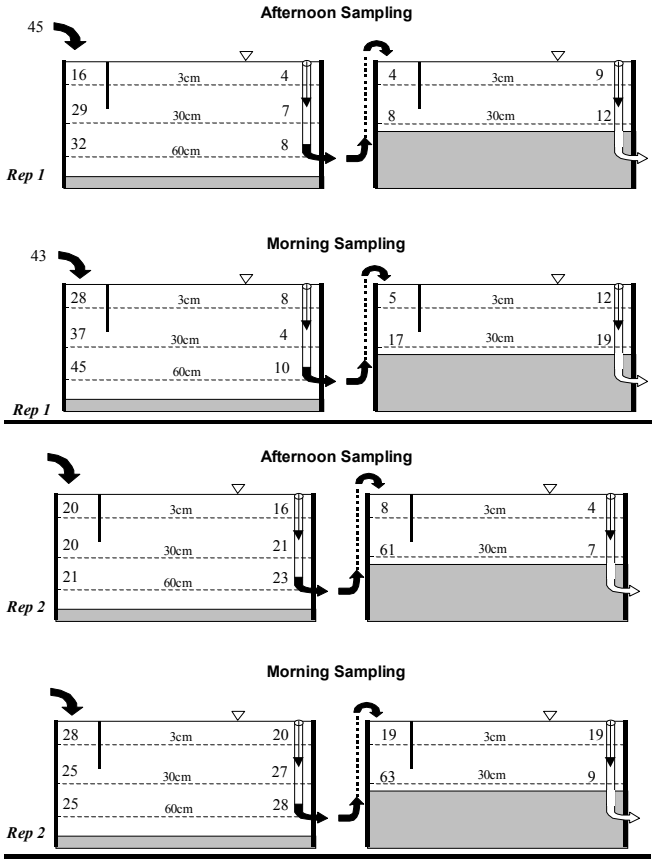

Figure 14. Soluble reactive phosphorus concentrations (µg/L) profiles during the Spatial-Temporal study on September 23-24, 1999 in the Sequential SAV mesocosms.

The dissolved oxygen (D.O.) concentration profiles followed a pattern that was similar to the static depth mesocosms, except that there were frequent instances of depressed surface D.O. concentrations during the daytime in the sequential mesocosms. Supersaturation was typical at these stations in the static depth mesocosms (cf. Figure 3 and Figure 15). Redox potentials, which were measured 46 days later for both experiments (static depth and sequential), demonstrated

more reduced conditions in the sequential mesocosms than in the static depth mesocosms, especially in the bottom waters (cf. Figure 4 and Figure 16).

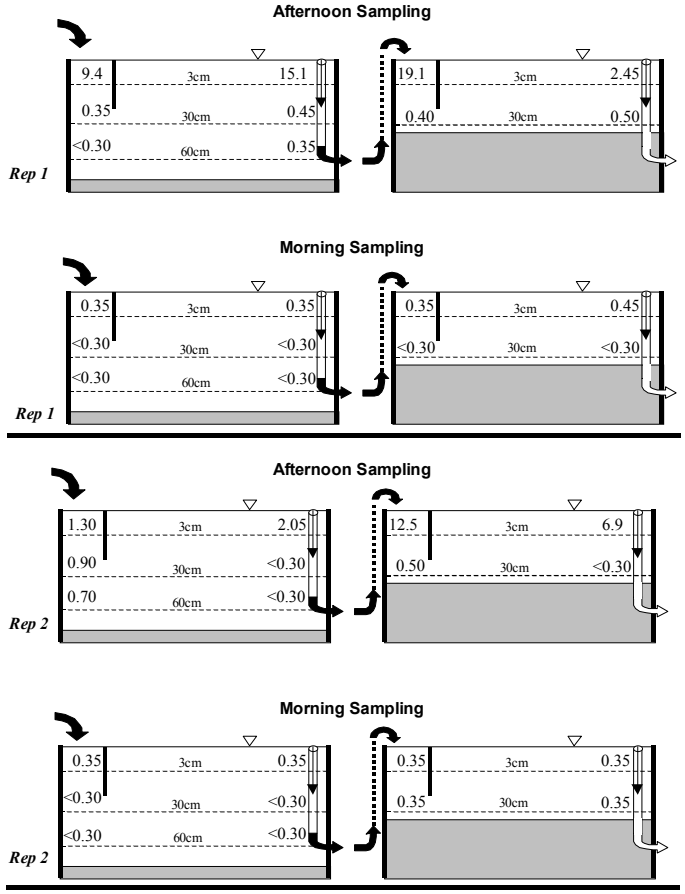

Figure 15. Dissolved oxygen (mg/L) profiles during the Spatial-Temporal study on September 23-24, 1999 in the Sequential SAV mesocosms.

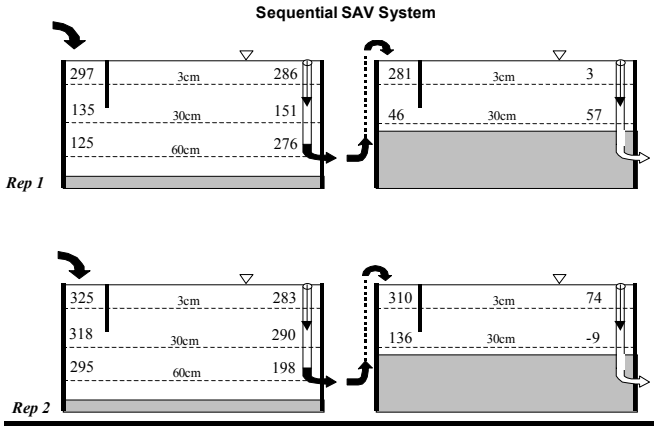

Figure 16. Mean values for daytime Eh (mV) profiles on November 10, 1999 in the Sequential SAV mesocosms.

Daytime dissolved Ca and alkalinity levels between the duplicate treatment trains diverged in a manner similar to pH values (cf. Figure 17- Figure 19). For the first replicate of the sequential treatment train, daytime surface pH values were considerably higher in three of the four stations than they were for the respective stations of the second replicate treatment train (Figure 17). Calcium concentrations were markedly reduced at those stations where the daytime pH values exceeded 8.5, as compared to the dissolved Ca levels at the other stations where pH values were more in the mid-7 range during both daytime and nighttime. As in the static water depth mesocosms, calcium precipitation as a carbonate, induced by a photosynthetic rise in the pH, is the likely explanation for this relationship.

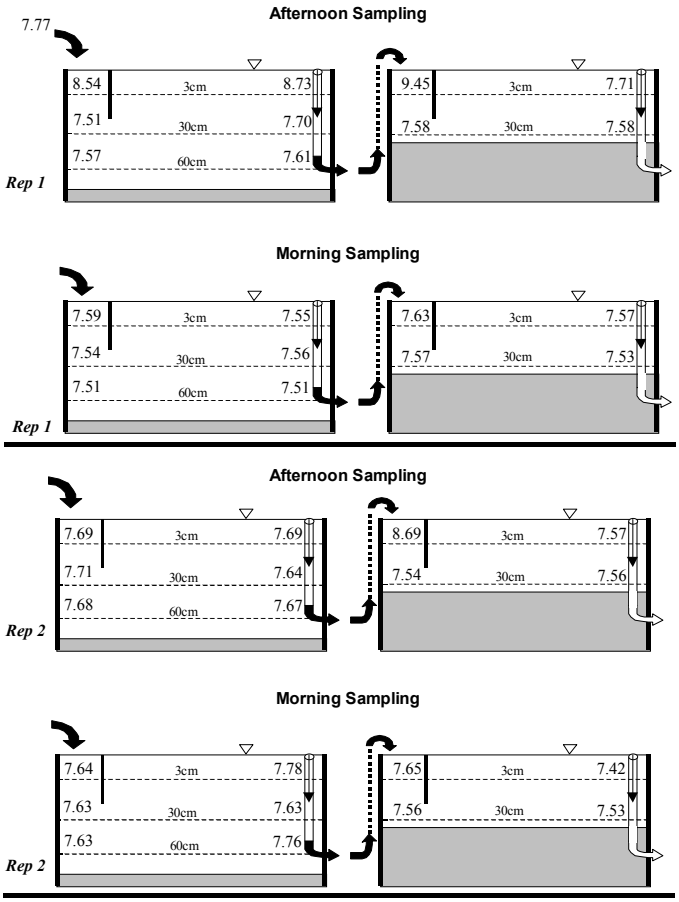

Figure 17. pH profiles during the Spatial-Temporal study on September 23-24, 1999 in the Sequential SAV mesocosms.

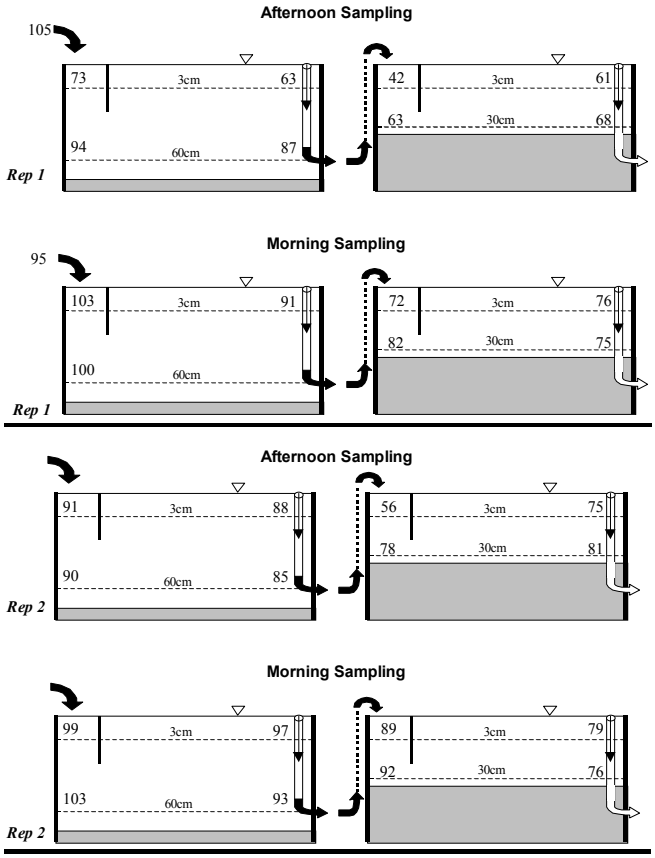

Figure 18. Dissolved calcium concentration (mg/L) profiles during the Spatial-Temporal study on September 23-24, 1999 in the Sequential SAV mesocosms.

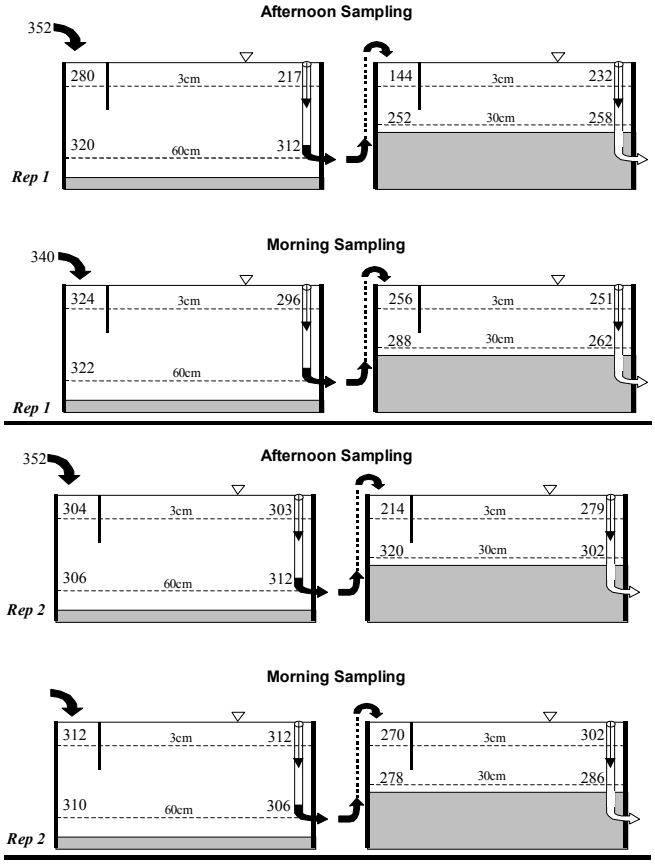

Figure 19. Alkalinity concentration (mg $CaCO_3$/L) profiles during the Spatial-Temporal study on September 23-24, 1999 in the Sequential SAV mesocosms.

Daytime correlations among pH, calcium and SRP concentrations for surface waters in the static depth mesocosms were much stronger than those for the sequential mesocosms. The r^2-values for daytime pH vs. Ca and Ca vs. SRP concentrations were 0.19 and 0.57, respectively, for the surface water stations of the sequential mesocosms. This implies that P coprecipitation with calcium carbonate may not be as prominent of a removal mechanism for P as it was in the static depth mesocosms.

Prior to these measurements in the sequential mesocosms, the SAV standing crop had exhibited a marked decline. Visual observations of the dominant SAV species (*Chara)* indicated a stressed condition, where most of the macroalga was either necrotic or chlorotic. Sulfide odor was noticeable, and in some areas of the mesocosms a filamentous blue-green alga (i.e., *Lyngbya* and *Oscillatoria*) formed contiguous surface and subsurface mats.

The aggregated water quality data suggest that decomposition rates were high in the sequential SAV mesocosms. Rapid decomposition of this SAV detritus would result in a community metabolism where respiration exceeds primary production, which in turn would lead to the observed low pH values, redox potentials, and D.O. concentrations, and the high SRP and Ca levels. The high temperatures (Figure 20) would further contribute to reduced D.O. concentrations.

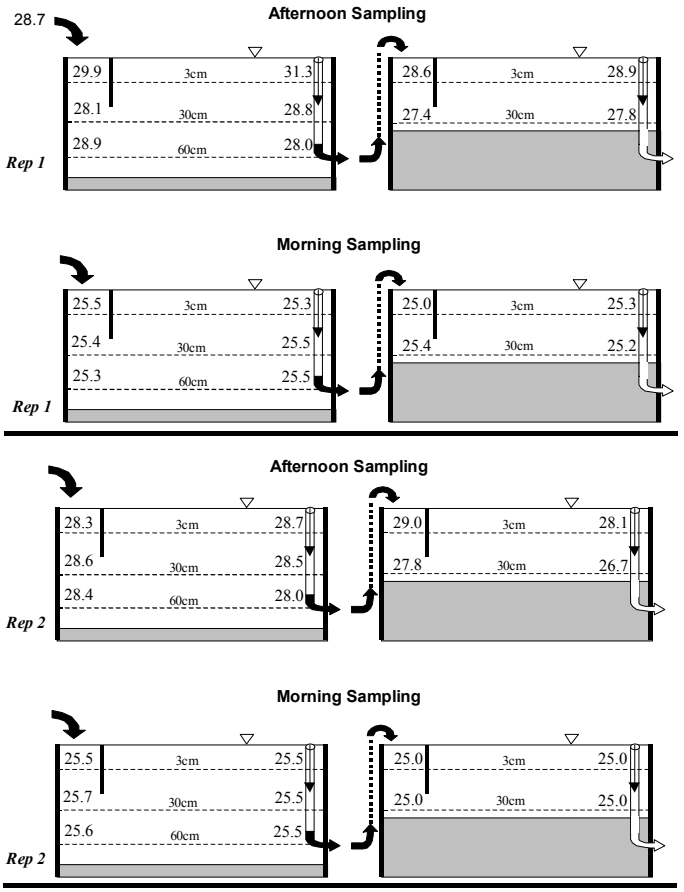

Figure 20. Temperature (°C) profiles during the Spatial-Temporal study on September 23-24, 1999, in the Sequential SAV mesocosms.

Phosphorus Removal in the Cattail-Dominated Mesocosms

During our Phase I study, we established cattail (*Typha*)-dominated mesocosms (in duplicate), to provide a comparison to the performance of the SAV mesocosms. Each of the two cattail mesocosms has exhibited different P removal efficiencies (Figure 21). The mesocosm providing less efficient P removal is covered with more duckweed (*Lemna*) and contains less SAV (*Najas*) than the other, suggesting that the difference in the densities of those species is contributing to differences in P removal. The variable plant community composition may affect light penetration into the water column, decomposition rates, substrate quality, and/or rate of P uptake by the plants themselves. One or more of these factors may explain mechanistically the differences in the P removal efficiencies. The higher effluent concentrations in January 2000 for both mesocosms are probably due to the higher P loadings during that month (see Figure 11).

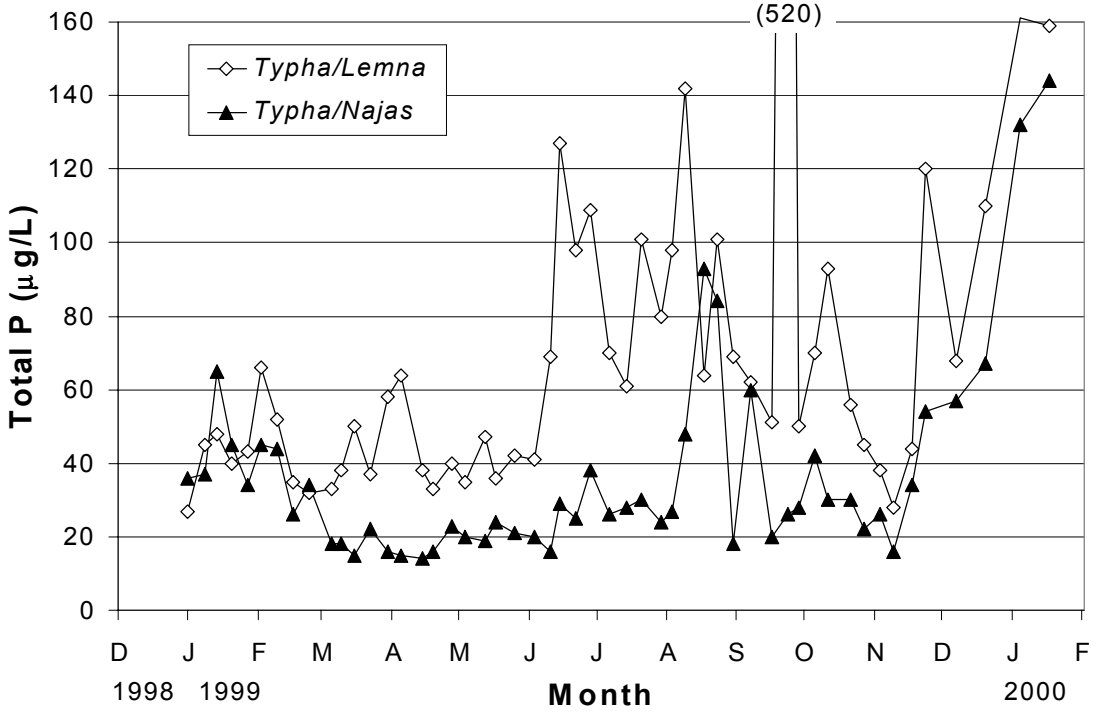

Figure 21. Total P concentration in the effluents of two mesocosms dominated by a mixed community of *Typha*, *Najas* and *Lemna*.

Long-term Phosphorus Removal in Shallow, Low Velocity Systems (Subtask 5vii)

We have operated shallow, low velocity raceways at the South Supplemental Technology site since summer 1998. Recently (December 1999 - February 2000), effluent TP concentrations in these SAV/periphyton raceways (9 cm deep) have periodically exceeded 10 µg/L, a benchmark that had been maintained since the beginning of data collection. This slight elevation in the effluent TP concentrations during this period likely occurred in response to a nearly two-fold increase in influent P concentrations (and loadings) (Figure 22). The outflow region LR bed has typically reduced raceway effluent TP levels by about 1-3 µg/L, such that the final discharge from the SAV/periphyton/LR system has remained below 10 µg/L. The overall (period of record) average TP concentrations for inflow, raceway and LR effluents have been 18, 10, and 8 µg/L, respectively.

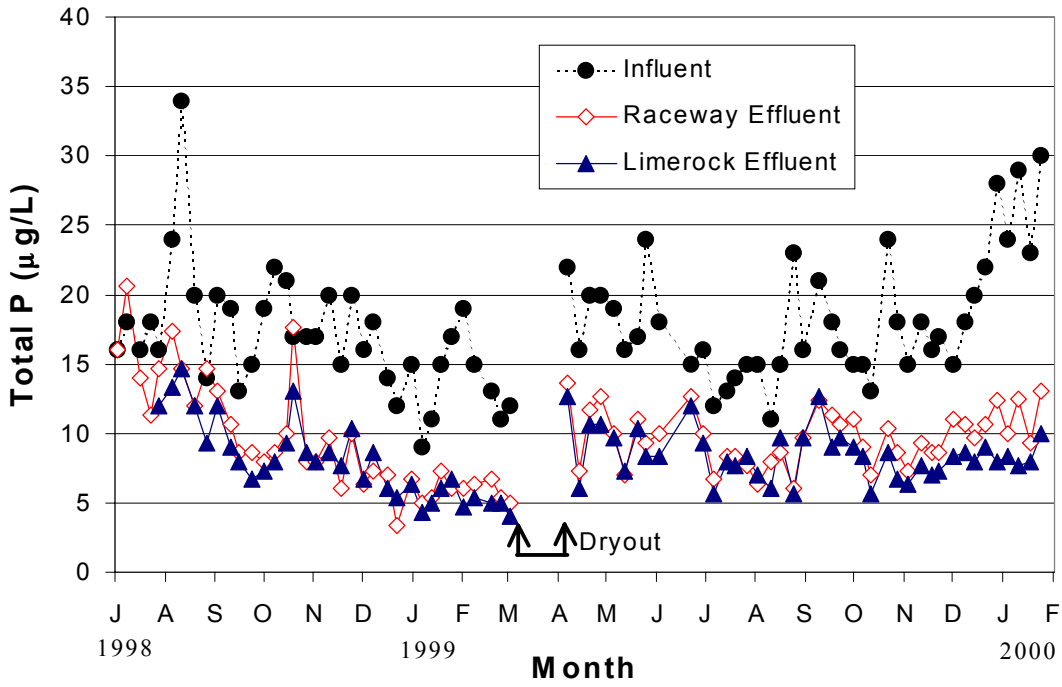

Figure 22. Total P concentrations in the influent and effluent of shallow, low velocity, SAV/periphyton raceways, and in the effluent of the subsequent limerock beds. Each value represents the mean of three replicate raceways and limerock beds.

Growth of SAV in Post-STA Waters on Muck, Limerock and Sand Substrates (Subtask 5ix)

In this study, SAV is being cultured on muck, limerock and sand substrates using STA-1W outflow (Post-STA) waters. To date, the SAV in the muck is providing slightly lower effluent TP concentrations than SAV cultured on the other substrates (Table 3). During the November to January quarter, more P was removed (relative to the inflow loading) in the muck substrate mesocosms than in previous months, which may have been a direct result of increased P loadings in the source water (Figure 23).

The SAV standing crop on the muck substrate appears more robust than the SAV in either the sand or limerock substrate mesocosms. The apparent superior nutritional status of the SAV in the muck systems may be enhancing water column P removal either directly (through plant P uptake) or indirectly (altering water chemistry). We plan to reduce hydraulic loading to these mesocosms in March 2000 to further investigate performance differences between substrates at low P loadings.

Table 3. Mean and range of total P concentrations (µg/L) from July 1999 to February 2000 for the influent and effluents of mesocosms containing limerock, muck and sand substrates. Each substrate treatment consists of duplicate mesocosms operated at a 1.3 day HRT.

	Influent	Limerock	Muck	Sand
mean	17	14	13	15
min.	9	6	6	10
max.	30	27	21	25

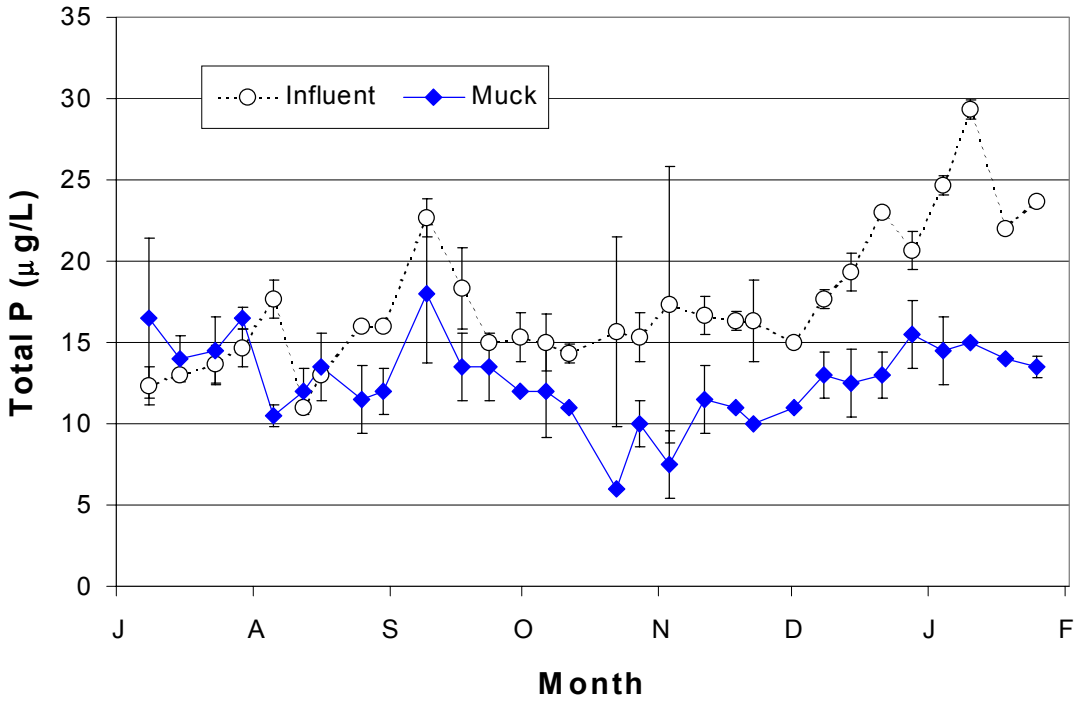

Figure 23. Total P concentrations in the influent (n=3) and effluent (n=2) of SAV mesocosms established on muck substrates. Error bars = ± 1 s.d.

Task 5 References

DB Environmental Laboratories (DBEL). 1999. A Demonstration of Submerged Aquatic Vegetation/Limerock Treatment System Technology for Removing Phosphorus from Everglades Agricultural Area Waters. Final Report submitted to the South Florida Water Management District and the Florida Department of Environmental Protection. West Palm Beach, FL.

Task 6. Test Cell Investigations

We performed two tracer studies in this task to further our understanding of the hydraulic characteristics (e.g., flow path, detention behavior, nominal vs. actual retention times, dispersion) of test cells dominated by SAV. These data will facilitate our interpretation of the P removal efficiencies of various wetland configurations (e.g., as a function of water depth, HLR, HRT, SAV density) and also help provide insight into P removal processes (e.g., chemical precipitation and adsorption, biological uptake), which are likely strongly influenced by hydraulic characteristics.

The discussion of tracer results in our Second Monthly Report (DBEL, 2000a) was limited to the tracer response curves, mass balances, and detention times from only the first dye study. A complete hydraulic analysis of both dye studies is provided in the following sections.

Methodology of the First Tracer Study

The first tracer study on October 26 - November 30, 1999 was designed to examine vertical (depth-related) short-circuiting on key hydraulic efficiency parameters (e.g., HRT and dispersion). All four of the SAV-dominated test cells (two North Test Cells: NTC-1 and NTC-15; two South Test Cells: STC-4 and STC-9) were utilized. To achieve the desired depths in the first dye study, water surface levels in all four test cells were lowered on October 10, 1999 from the operational depth of approximately 1.1 m that had been maintained at for five months prior. The water column depths of two of the test cells (NTC-15 and STC-4) were set at 0.5 m each; the remaining two test cells (NTC-1 and STC-9) were deeper (0.91 m and 0.79 m respectively). The hydraulic loading rates (HLR) in all four test cells were increased from the historic 3 cm/day loading and maintained within a narrow range of 10-13 cm/day throughout the study. At the time of the tracer study, the dominant SAV were *Chara* in the two North Test Cells (NTC-1 and NTC-15) and *Hydrilla* in the two South Test Cells (STC-4 and STC-9). Descriptions of prior and modified hydraulics, site preparation work (e.g., flow and depth alterations; installation of influent distribution manifolds); and the hydrologic calibrations, error analyses, and final hydraulic parameters to the test cells were reported by DBEL in the First Monthly Report (DBEL, 2000b). Biological and hydrological conditions for each of the test cells during the first tracer study, as well as methodologies associated with tracer injection, sampling, laboratory dye analysis, and computations of key

hydraulic efficiency parameters (i.e., HRT, dispersion, "tanks-in-series" number (N), and the Peclet number (Pe)), were presented in the Second Monthly Report (DBEL, 2000a).

Methodology of the Second Tracer Study

Only the two North Test Cells (NTC-1 and NTC-15) were used for the second tracer study (December 16, 1999 to February 1, 2000). In this experiment, we assessed the effect of HLR-driven short-circuiting on hydraulic efficiency. Flow to the 0.8 m deep NTC-1 was quadrupled on December 9, 1999, to simulate a pulse load of runoff. On the same date the depth of NTC-15 was increased from 0.5 to 0.84 m, to assess the effects of a rapid stage increase on hydraulic performance.

Tracer Injection

The amounts of 20% Rhodamine-WT dye added to the influent manifolds of NTC-1 and NTC-15 on December 16, 1999, were 113.6 and 103.3 g, respectively. The tracer was applied in 3.8-L volumes over a one-minute time span to each test cell.

Sampling Frequency

Samples were collected from the NTC-15 effluent weir location at the following frequencies: 6 times per day (every 4 hours) for the first 4 days; 3 times per day (every 8 hours) for the next two days; twice daily for the next 5 days; daily for the next 10 days; and finally twice a week for the next 3.5 weeks. The same sampling schedule was followed for NTC-1 through the 14th day. Daily samples were then collected for only 3 days (instead of 10 days) at NTC-1, with the final sample taken 4 days after the last daily sample.

Laboratory Analysis of Dye Tracer

Rhodamine-WT concentrations were measured on a Turner Designs Model 10-AU-005-CE fluorometer with excitation and emission filters of 550 and > 570 nm, respectively (Wilson et al. 1986). The emission filter consisted of an orange sharp-cut filter. A reference filter (>535 nm) reduced baseline drift and instrument noise by filtering out scattered light. The light source was a clear quartz lamp. The standard curve was linear to 80 mg/L and the method detection limit was 0.1 µg/L. Since Rhodamine-WT fluorescence is sensitive to temperature, both standards

and samples were analyzed at room temperature. Background fluorescence (from dissolved organic matter) was subtracted from each of the sample fluorescence readings. Prior to analysis, all water samples were stored in amber-colored bottles.

Computations for Determining Hydraulic Parameters

Calculations for determining selected hydraulic parameters for the test cells, based on the tracer data, were performed as follows.

The nominal HRT, τ, is the ratio of the volume of water in the treatment wetland (V) divided by the volumetric flow rate of water (Q):

$$\tau = V/Q \quad (1)$$

The tracer residence time, τ_a, is defined as the average time that a tracer particle spends in Cell 4, and is the first moment of the residence time distribution (RTD) function. The RTD represents the time various fractions of water spend in the test cells. It is the contact time distribution for the system (Kadlec 1994). The RTD defines the key parameters that characterize the actual detention time. Levenspiel (1989) uses the RTD in the analysis of reactor behavior.

The mean residence time, τ_a, was calculated by dividing Eq. 4 of the tracer flow distribution, by Eq. 3, both of which are based on mean outflow rates and tracer concentrations (Kadlec 1994):

$$\tau_a = M_1/M_0 \quad (2)$$

$$M_0 = \int_0^{t_f} Q_e(t)\,C(t)\,dt \quad (3)$$

$$M_1 = \int_0^{t_f} tQ_e(t)\,C(t)\,dt \quad (4)$$

where C(t)=exit tracer concentration (mg/m^3); Q_e = flow rate (m^3/day); t = time (days); and t_f = total time span of the outflow pulse (days).

To find the RTD, the concentration response curve (experimental C(t) vs. t curve) is converted to an E_t curve by changing the concentration scale so that the area under the response curve is unity (Levenspiel 1989). This is accomplished by multiplying the concentration readings by the volumetric flow rate divided by the mass (M) of injected tracer:

$$E_t = C(Q_e/M) \quad (5)$$

where E_t = RTD function in reciprocal time units.

The RTD function is normalized when it is expressed in terms of the dimensionless time scale by multiplying the Y-axis (i.e., the E_t function) units by τ (the nominal HRT):

$$E_\Theta = \tau E_t \quad (6)$$

where E_Θ= dimensionless RTD function,

and dividing the time units of the X-axis by τ:

$$\Theta = t/\tau \quad (7)$$

where Θ = dimensionless time scale and represents the number of mean HRTs.

This changes the X and Y axes so that the area under the curve is still equal to one, but the Y and X axes are normalized to τ (Levenspiel 1972). The purpose of creating the normalized distribution function, E_Θ, is to be able to compare the flow performance among wetlands of different sizes and containing different plant communities and densities.

Whereas τ_a represents the centriod of the distribution and is the first moment of the RTD, the variance (σ^2) is the square of the spread of the distribution, or a measure of the dispersive processes, and is expressed in units of (time)^2:

$$\sigma^2 = \frac{\int_0^{t_f} t^2 Q_e(t) C(t) dt}{\int_0^{t_f} Q_e(t) C(t) dt} - \tau_a^2 \quad (8)$$

The variance, which is the second moment of the RTD, is particularly useful for matching experimental curves to one of a family of theoretical curves (Levenspiel 1972).

The variance can be rendered unitless by dividing by the square of the tracer detention time:

$$\sigma_\Theta^2 = \frac{\sigma^2}{\tau_a^2} \quad (9)$$

where σ_Θ^2 is the dimensionless variance of the tracer pulse.

Two common one-parameter models used to characterize non-ideal flows are the tank-in-series (TIS) and dispersion models (Levenspiel 1972). The TIS model views flow through a series of

equal-size ideal stirred tanks, and the one parameter in this model is the number of tanks (N) in the chain. The number of constantly stirred tanks in the series that best matches the tracer response curve is given by N, which is determined by:

$$N = \frac{1}{\sigma^2_\theta} \tag{10}$$

To construct an idealized dimensionless tracer response curve for N = 1, 2, etc.:

$$E_\Theta = \frac{N}{(N-1)!}(N\frac{t}{\tau_a})^{N-1} e^{-N\frac{t}{\tau_a}} \tag{11}$$

The second model is a dispersed plug flow, or dispersion model, which draws on an analogy between mixing in actual flow and a diffusional process. Here the dispersion process is superimposed on a plug flow model, and mixing is presumed to follow a diffusion equation (Kadlec and Knight 1996). For boundary conditions that are closed-closed, the following relation for the dimensionless variance has been found (Fogler 1992):

$$\sigma^2_\Theta = \frac{2}{Pe} - \frac{2}{Pe^2}(1 - e^{-Pe}) \tag{12}$$

where Pe is the Peclet number, dimensionless.

Eq (12) can be converted to the wetland dispersion number ($\mathfrak{D}$, dimensionless) by utilizing:

$$\mathfrak{D} = \frac{D}{uL} = \frac{1}{Pe} \tag{13}$$

where L = distance form inlet to outlet, m

u = superficial velocity, m/day

D = dispersion constant, m²/day

Combining Eqs. (12) and (13) yields:

$$\sigma^2_\Theta = 2\mathfrak{D} - 2\mathfrak{D}^2(1 - e^{-\frac{1}{\mathfrak{D}}}) \tag{14}$$

Results of the Two Dye Studies

Tracer Response Curves

The concentration response curves for the test cells exhibited non-ideal flow distributions, where neither plug flow reactor (PFR) nor constantly stirred tank reactor (CSTR) flow patterns occurred (Figure 24 - Figure 26). For all test cells that received a HLR of 10 - 13 cm/day, the tracer appeared at the effluent regions sooner than expected, based on the nominal HRTs. We observed lags ranging from 0.5 to 2.5 days before the maximum tracer concentration reached the effluent region of the cells (Figure 24 - Figure 26). After the lag periods, the ascending limb of the tracer curve in 3 of the test cells peaked close to the maximum concentrations (36 - 44 µg/L) expected for CSTR behavior (Figure 24a and Figure 25a and b).

The effects of a quadrupling of the HLR in NTC-1 during the second tracer study resulted in a profile for well-mixed hydraulics (Figure 27). Unfortunately, the increased velocity caused some of the biota to be exported from the test cell, which subsequently was trapped on the discharge weir screen. The blockage reduced the discharge flow early during the study, thereby compromising the outflow data to such an extent that calculations for determining tracer recovery, mean HRT (τ_a) and variance (σ^2) could not be performed.

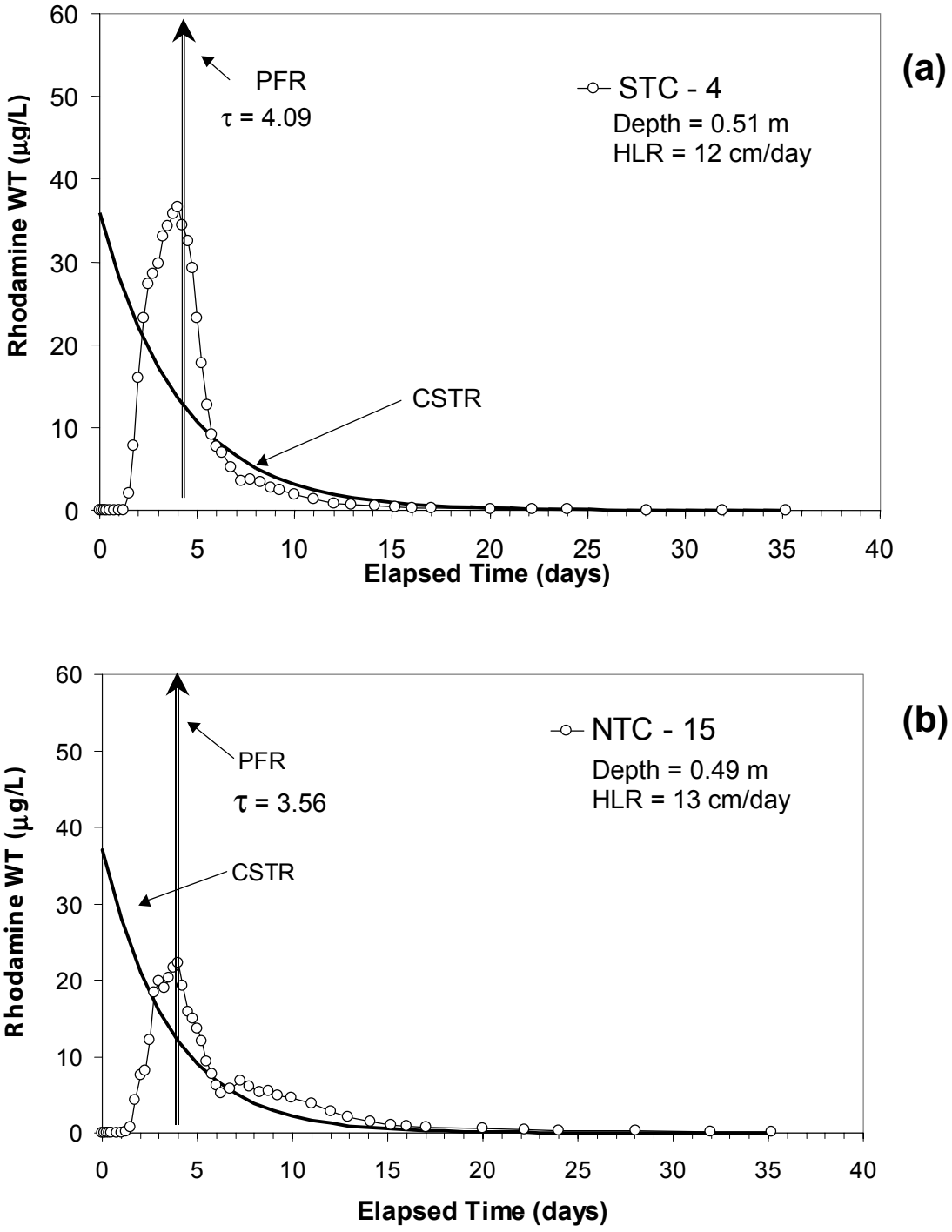

Figure 24. Tracer response curves for the fluorescent dye Rhodamine-WT applied to the shallow test cells during the first tracer study. Graph (a) reflects the South Test Cell (STC-4) and graph (b) reflects the North Test Cell (NTC-15). Responses to ideal well-mixed (CSTR) and plug flow (PFR) conditions are represented by the exponential decay and vertical (coinciding with the nominal HRT, τ) lines.

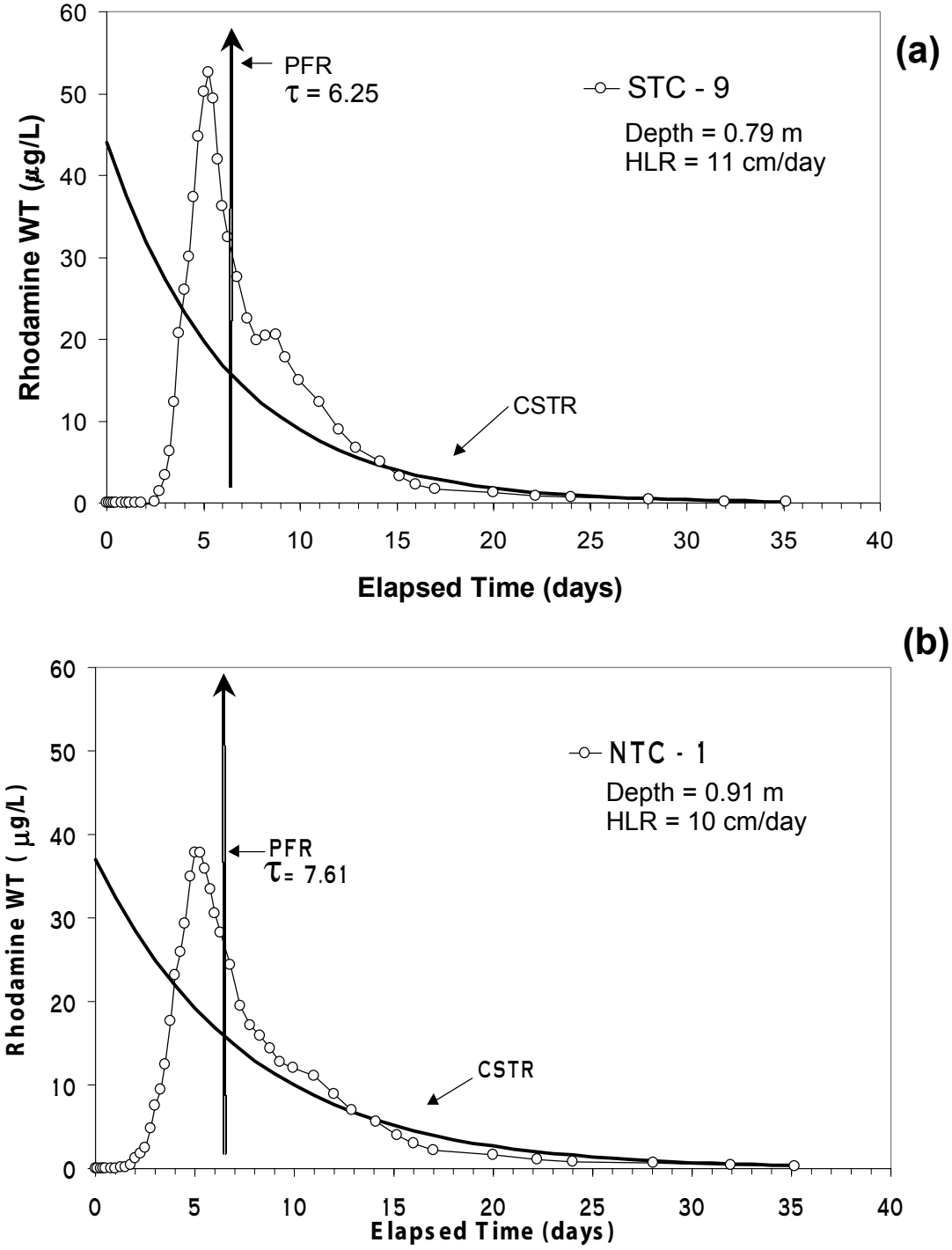

Figure 25. Tracer response curves for the fluorescent dye Rhodamine-WT applied to the deeper test cells during the first tracer study. Graph (a) reflects the South Test Cell (STC) and graph (b) reflects the North Test Cell (NTC-1). Responses to ideal well-mixed (CSTR) and plug flow (PFR) conditions are represented by the exponential decay and vertical (coinciding with the nominal HRT, τ) lines.

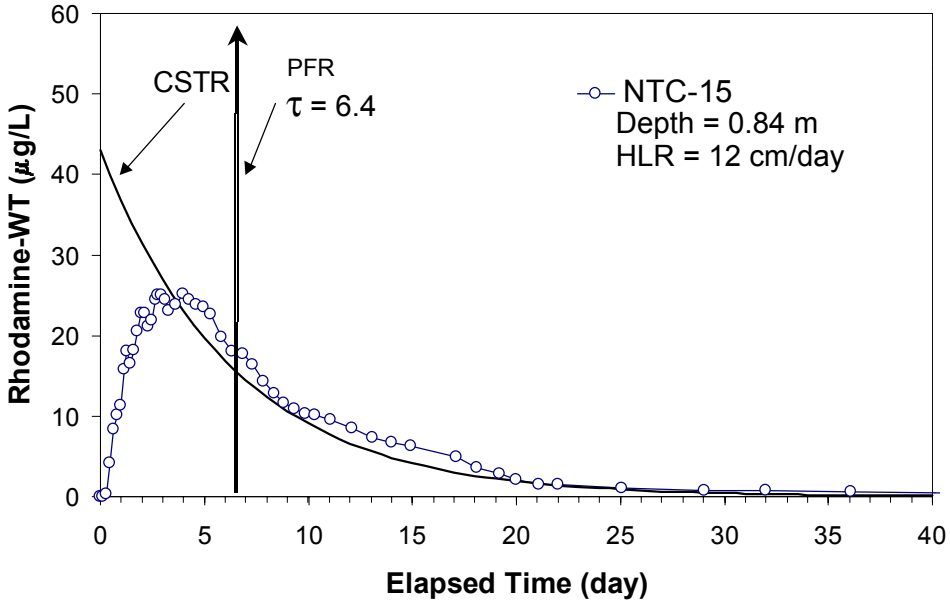

Figure 26. Tracer response curve for the fluorescent dye Rhodamine-WT applied to a deep test cell during the second tracer study. Responses to ideal well-mixed (CSTR) and plug flow (PFR) conditions are represented by the exponential decay and vertical (coinciding with the nominal HRT, τ) lines.

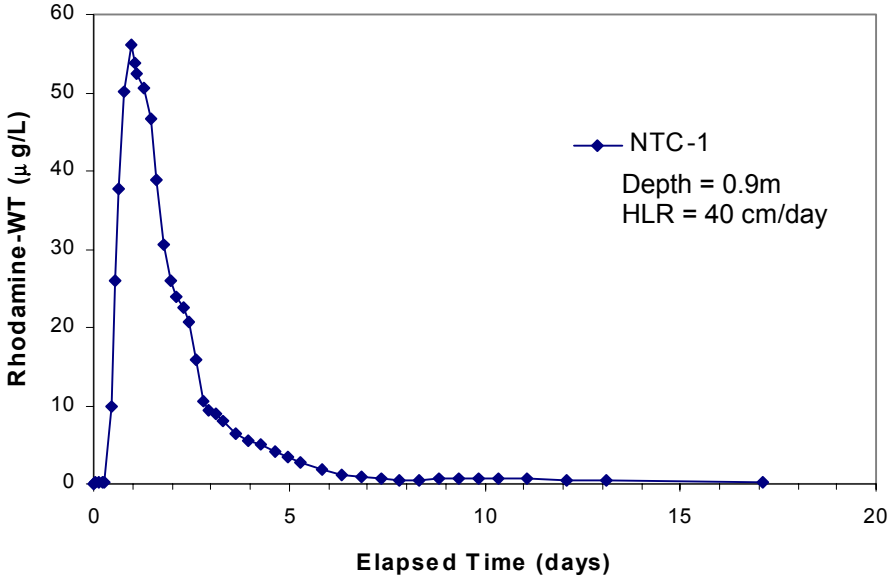

Figure 27. Tracer response curve for the fluorescent dye Rhodamine-WT applied to NTC-1 during the second tracer study.

Tracer Mass Balances

The Rhodamine-WT mass balances were calculated by comparing the injected tracer mass to the tracer mass detected at the effluent. The total mass of tracer exiting the SAV test cells is given by Eq. 3. A comparison of the recovered tracer mass and the amount injected to each test cell demonstrates a good recovery for Rhodamine-WT, with higher recoveries associated with the South Test Cells (Table 4).

Table 4. Comparison of recovered dye mass with the dye amounts injected to test cells operated at two different water depths during two separate dye investigations.

Dye Study Investigation	Test Cell Designation	Depth (m)	HLR (cm/day)	Mass Injected (g)	Mass Recovered (g)	% Recovery
No. 1	NTC-1	0.91	10	75.9	59.4	78
No. 1	NTC-15	0.49	13	44.0	35.3	80
No. 1	STC-4	0.51	12	44.0	39.5	90
No. 1	STC-9	0.79	11	88.0	77.7	88
No. 2	NTC-15	0.84	12	103.3	81.8	79

Tracer Detention Time

Our data show that the tracer detention time (τ_a) was slightly longer than the nominal detention time (τ) in all the test cells (Table 5). This suggests there may have been some inaccuracies associated with the flow, mass, or volume (particularly depth) measurements. Given the careful measurements of injection mass and flow, we suspect that cell volume (inconsistent bottom substrate elevations) or vegetation effects likely accounts for the disparity between the measured and nominal HRTs.

Table 5. Comparison of nominal (τ) and measured (τ_a) hydraulic retention times for four test cell during two separate dye trace investigations.

Dye Study Investigation	Test Cell Designation	Depth (m)	HLR (cm/day)	τ (days)	τ_a (days)	τ_a/τ
No. 1	NTC-1	0.91	10	7.6	8.6	1.13
No. 1	NTC-15	0.49	13	3.6	6.9	1.92
No. 1	STC-4	0.51	12	4.1	4.7	1.15
No. 1	STC-9	0.79	11	6.25	8.0	1.29
No. 2	NTC-15	0.84	12	6.4	8.9	1.39

Hydraulic Efficiency

Figure 28 shows a comparison of the dimensionless RTD functions (E_Θ) from the four test cells during the first and second dye studies. Table 6 shows a comparison of calculated hydraulic parameters from the dye studies.

The tanks-in-series (TIS) model is a commonly used technique for comparing the hydraulic efficiency of different wetlands. It compares the dimensionless RTD function (E_Θ) of a wetland with the theoretical RTD functions of increasing tanks-in-series (TIS) according to Eq. 10. Special cases of the TIS are the single CSTR (N=1) and the PFR (N=4). In other words, the higher N that a wetland represents, the closer it resembles a PFR and less of a CSTR. Hydraulic characteristics of a PFR are more conducive to more efficient treatment of P since the average time that inflow water is retained in the wetland more closely approaches the HRT; or alternatively, a lesser proportion of the inflow water leaves the wetland early.

The calculated TIS values for the test cells lie between 1.35 and 3.3 (Table 6). Kadlec and Knight (1996) report a typical range of 2 < N < 8 for treatment wetlands; three of the five TIS values for SAV dominated test cells fall within this range.

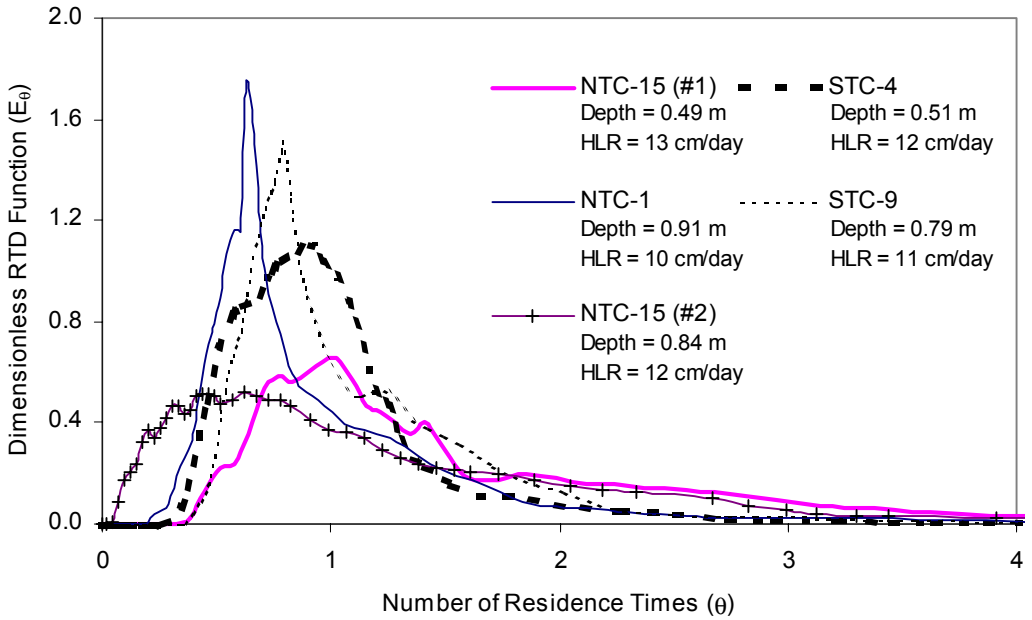

Figure 28. Dimensionless residence time distribution (RTD) functions for five test cells during the first and second tracer investigations. The two shallower (0.5 m) test cells (NTC-15 #1 and STC-4) had nominal hydraulic retention times of 3.6 - 4.1 days; the three deeper (0.8 - 0.9 m) test cells (NTC-1, NTC-15 #2, and STC-9) had nominal HRTs of 6.3 - 7.6 days.

A second parameter used to compare hydraulic performance between wetlands is the wetland dispersion number, ℑ, which is a parameter in a dispersed plug flow model. The dispersion number is calculated as the dispersion coefficient divided by the product of the superficial velocity and length of the wetland (D/[uL] in Eq. 13) and describes the ratio of the rate of tracer transport by diffusion or dispersion to convection (bulk flow). Alternately, the Peclet number, Pe, which is the inverse of the dispersion number (Eq. 10), represents the ratio of convection (bulk flow) to transport by diffusion or dispersion processes.

Kadlec (1999) states that values of ℑ range from 0.2 to 0.4 in wetlands (predominantly emergent macrophyte wetlands), which places them in the "large amount of dispersion" category. The ℑ values obtained for the four SAV-dominated test cells in the first dye study are mostly within that range (Table 6). Although there was some overlap in ℑ between the shallow and deep test cells, the deep test cells were more hydraulically efficient than the shallow test cells.

Table 6. Comparison of key hydraulic parameters among four test cells during the first and second dye studies.

Wetland Cell Designation	Water Depth (m)	Nominal HRT τ, days	Measured HRT τ_a, days	Variance σ^2, day^2	Dimensionless Variance σ_θ^2	Tanks-in-Series N	Wetland Dispersion Number ℑ	Peclet Number Pe
NTC-15	0.49	3.6	6.9	28.4	0.60	1.7	0.56	1.79
STC-4	0.51	4.1	4.7	8.4	0.40	2.6	0.27	3.70
NTC-1	0.91	7.6	8.6	29.1	0.39	2.5	0.26	3.85
STC-9	0.79	6.3	8.0	19.3	0.30	3.3	0.18	5.55
NTC-15*	0.84	6.4	8.9	58.5	0.74	1.35	1.00	1.00

* second dye study

The range of values for dispersion and Peclet numbers (Table 6) indicates that transport within the four SAV dominated test cells was controlled mainly by bulk flow (ℑ < 1, Pe > 1) during the first dye study, but that transport processes in NTC-15 during the second dye study were equally proportioned between bulk flow and dispersion. Considering that hydraulic efficiency in treatment wetlands is thought to be enhanced by plug flow rather than dispersive or diffusive flow processes, then some of the test cells (i.e. STC-9) performed better than others (i.e. NTC-15 in the first and second dye studies) from a hydraulic perspective.

The results from the first dye study, where duplicate sets of shallow (0.5 m) and deep (0.8 and 0.9 m) SAV-dominated cells were tested, showed near equality in the σ_Θ^2, N, D, and Pe for one deep and one shallow treatment (NTC-1 and STC-4 in Table 6). However, there was at least a two-fold difference in these hydraulic parameters between the other pair of deep and shallow test cells, with the deeper cell (STC-9) expressing more plug flow than the shallower (NTC-15). This finding is contradictory to what we would have expected, based on the test cell antecedent conditions (maintained at 1.1 m deep for 5 previous months) and modifications to the test cells prior to this study (lowering depth to values indicated in Table 6 within two weeks prior to study). Assuming that the test cells had equal volumetric SAV densities prior to stage changes, the shallow test cells would have had a more dense SAV community (on a volumetric basis) than the deeper cells, since the same biomass was occupying less volume of water. Nepf et. al (1997) and Kadlec (1993) both suggest a tendency towards decreased dispersion with increased vegetation density, however our findings (Table 6) for SAV systems suggest the opposite.

Figure 29 shows a comparison between the dimensionless RTD for NTC-15 after a decrease in stage (first dye study) and after an increase in stage (second dye study). We attribute the early breakthrough in the second dye study to vertical short-circuiting over top of the SAV community before the SAV expanded to occupy the entire water volume. Clearly, the effect of water stage change on hydraulic performance (Figure 29) is much more pronounced in SAV wetlands than in emergent macrophyte wetlands. We will investigate this phenomenon more closely in the "Fluctuating Depth" mesocosm experiment.

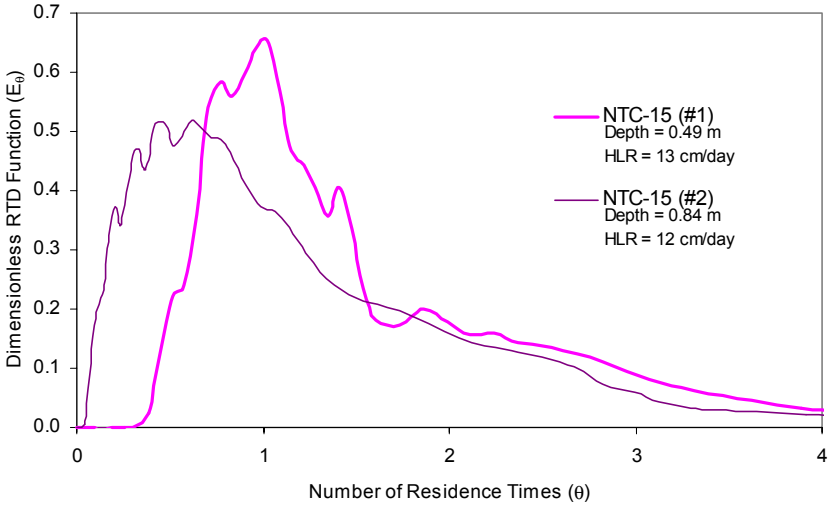

Figure 29. Dimensionless residence time distribution (RTD) functions for test cell NTC-15 at depths of 0.49 m (NTC-15 #1, τ=3.6 days) and 0.84 m (NTC-15 #2, τ=6.4 days) during the first and second tracer studies.

Test Cell Phosphorus Removal Performance

The two North Test Cells (NTC-1 and NTC-15) provided nearly identical P removals on a percentage basis (~70%), from September 1 until December 10, 1999. On this latter date, we provided a four-fold increase in the HLR (to 40 cm/day) to NTC-1 in preparation for the second tracer study. After this time, NTC-1 effluent P concentrations increased significantly, but NTC-15 continued to remove P at the same efficiency as it had previously (Figure 30).

Phosphorus removal efficiencies for both South Test Cells (Figure 31) were considerably poorer than for the North Test Cells (Table 7). It is likely that the P in the inflow to the South Test Cells is comprised of more recalcitrant forms (i.e., particulate P and DOP) than inflows to the Northern Test Cells. Moreover, *Hydrilla* dominates both of the South Test Cells and the P removal effectiveness of the SAV species is unknown.

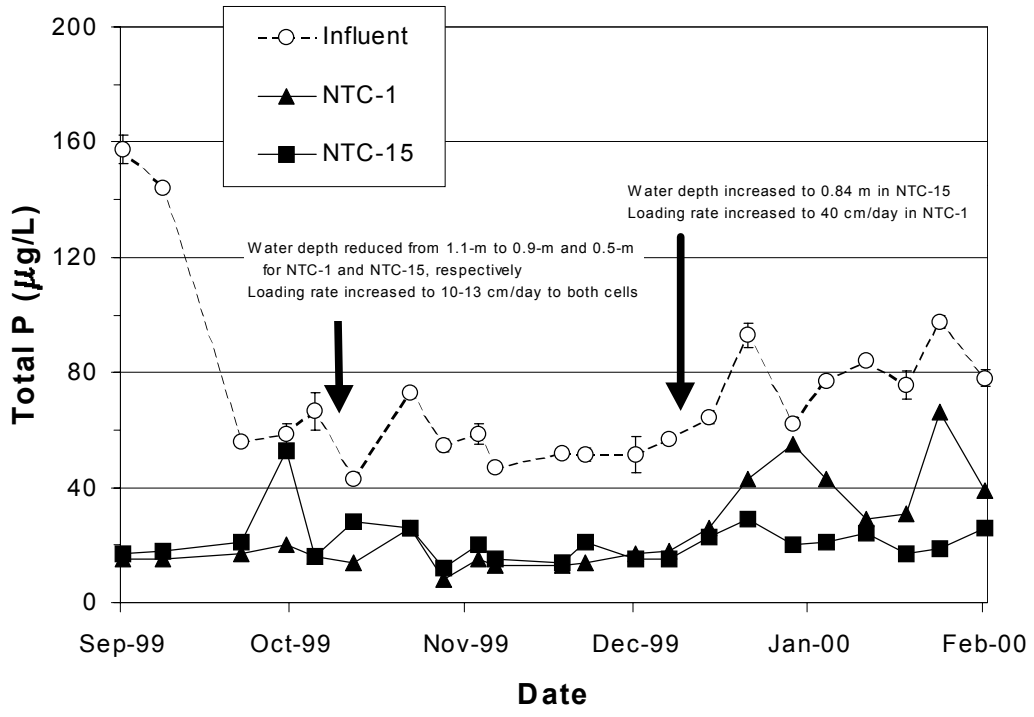

Figure 30. Total P concentrations in the influent and effluents of North Site Test Cells. Error bars for influent (n=2) represent ± 1 s.d.

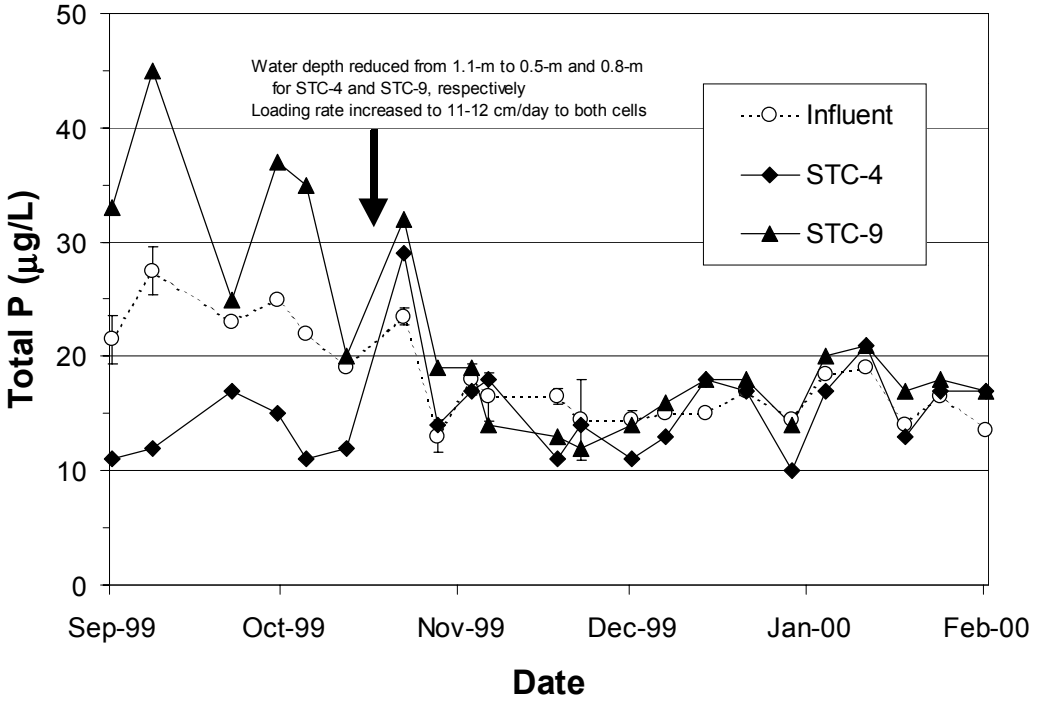

Figure 31. Total P concentrations in the influent and effluents of South Site Test Cells. Error bars for influent (n=2) represent ± 1 s.d.

Table 7. Mean influent and effluent total P concentrations (µg/L) from September 1, 1999 to February 1, 2000 for the North and South Test Cells.

		Influent	Effluent	% Removal
North Test Cells	NTC-1	72	25	65
	NTC-15	74	21	72
South Test Cells	STC-4	18	15	17
	STC-9	19	22	-17

Task 6 References

DB Environmental Laboratories (DBEL). 2000a. A Demonstration of Submerged Aquatic Vegetation/Limerock Treatment System Technology for Phosphorus Removal from Everglades Agricultural Area Waters: Follow-on Study. Second Monthly Report submitted to the South Florida Water Management District and the Florida Department of Environmental Protection. West Palm Beach, FL.

DB Environmental Laboratories (DBEL). 2000b. A Demonstration of Submerged Aquatic Vegetation/Limerock Treatment System Technology for Phosphorus Removal from Everglades Agricultural Area Waters: Follow-on Study. First Monthly Report submitted to the South Florida Water Management District and the Florida Department of Environmental Protection. West Palm Beach, FL.

Fogler, H.S. 1992. Elements of Chemical Reaction Engineering (2nd Ed.). Prentice-Hall, Inc., Englewood Cliffs, N.J.

Kadlec, R.H., W. Bastiaens, and D.T. Urban, 1993. Hydrological design of free water surface wetlands. In: G.A. Moshiri (ed.) Constructed Wetlands for Water Quality Improvement. Lewis Publishers, Boca Raton.

Kadlec, R.H. 1994. Detention and mixing in free water wetlands. Ecol. Engineering 3:345-380.

Kadlec , R.H., and R.L. Knight. 1996. Treatment Wetlands. CRC Lewis Publishers. Boca Raton, Fl.

Kadlec, R.H. 1999 The inadequacy of first-order treatment wetland models. Ecol. Eng. (in press).

Levenspiel, O. 1972. Chemical Reaction Engineering (2nd Ed.). John Wiley & Sons, Inc. New York.

Levenspiel, O. 1989. The Chemical Reactor Omnibook. Oregon State University Book Stores, Corvallis, Oregon 97339.

Nepf, H.M., C.G. Mugnier, and R.A. Zavistoski. 1997. The effects of vegetation on longitudinal dispersion. Estuarine, Coastal and Shelf Science. 44: 675-684.

Wilson, Jr., J.F., E.D. Cobb, and F.A. Kilpatrick. 1986. Fluorometric Procedures for Dye Tracing. U.S. Geological Survey Techniques of Water-Resources Investigations, Book 3, Chapt. A12, 34 p.

Task 9. Development of Performance Forecast Model

During this quarter, our efforts on this task focused on collecting and reviewing historic Cell 4 performance data and on initiating forecast model development. As a first step in model development, DBEL developed, programmed (in QBasic), and calibrated two lumped-parameter models based on Cell 4 data: a dynamic TP removal model and a parallel-path SRP and PP+DOP removal model. Simulated time histories of TP effluent are presented and compared to actual Cell 4 performance. Future efforts will use these programmed models as templates for developing a process-based SAV performance model.

Review of Historic Cell 4 Performance

Introduction

Cell 4 in STA-1W has been in continuous operation since mid-1994. We obtained and analyzed District-collected data of regularly measured Cell 4 hydrologic and water quality parameters. The Cell 4 performance database is important because it will be used for input/output files in dynamic simulation modeling and because it is an historical archive of the only known full-scale SAV-based treatment system.

Hydrologic Parameters

The hydrologic data available from the District were sufficient to construct daily water balances from January 1995 through April 1999 using measured inflows, measured outflows, measured rain events, and District-estimated seepage (through the western levee) and ET losses. Additionally, daily water storage in Cell 4 can be estimated using measured stage (at inflow and outflow levees and two internal stations) and a District-published stage-volume relationship.

Figure 32 summarizes the average partitioning of the Cell 4 water budget from May 1995 through April 1999. The water budget is dominated by G254 inflows and G256 outflows. However, estimated seepage outflows account for approximately 10% of the water leaving Cell 4. The 'Inflow' and 'Outflow' halves of the bar chart are balanced within 3%, indicating fairly

accurate District estimates of seepage and ET. Figure 33 shows time histories of the Cell 4 inflow, outflow and stages. Hydraulic loading rates were calculated from measured data assuming a 1.47E6 m² Cell 4 surface area. The historical average HLR in Cell 4 has been 16.2 cm/day, while the historical average outflow has been 15.0 cm/day. The average Cell 4 water depth has been 0.61 m.

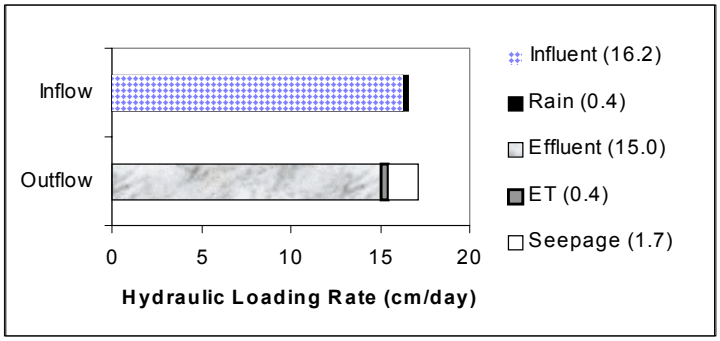

Figure 32. Average Cell 4 water budget over 4.3-years.

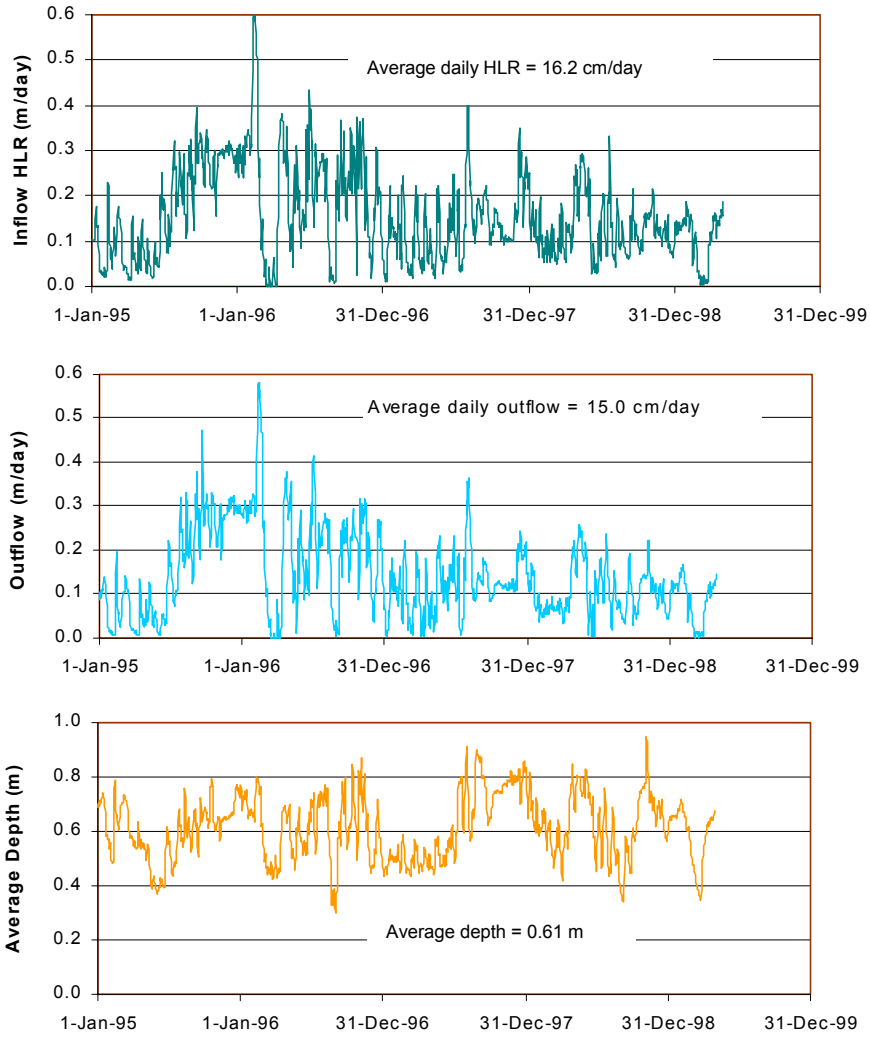

Figure 33. Time histories of Cell 4 hydrologic parameters.

Water Quality Parameters

The District performs regular water quality sampling at four Cell 4 locations: G254 inflow stations, G256 outflow stations, and the internal ENR401 and ENR402 stations that are located approximately one-thirds and two-thirds of the distance along Cell 4's length, respectively. With respect to likely SAV removal mechanisms, Cell 4 water quality parameters that are pertinent to simulation modeling include total phosphorus (TP), soluble reactive phosphorus (SRP), dissolved organic phosphorus (DOP), particulate phosphorus (PP), and calcium (Ca). Data on these water quality data were available from the District for the period of January 1995-mid-1999, but at a much coarser resolution than daily hydrologic data. The District has collected Cell 4 water quality data as weekly composites, biweekly grab samples, or monthly grab samples, depending upon the constituent and sampling location. Table 8 summarizes the District's sampling schedule for each constituent at each location. Weekly composite data for TP at G254 and G256 stations were collected with auto-samplers and were comprised of grab samples collected 3 times per day, 7 days per week. As indicated in Table 8, the District did not report PP and DOP measurements after 1997. We estimated PP and DOP after 1997 from TP, TDP (total dissolved phosphorus), and SRP data.

Table 8. Summary of District's Cell 4 Water Quality Sampling

Constituent	Period	G254	ENR401	ENR402	G256
Total Phosphorus	1995-1999	weekly comp. biweekly grab	monthly grab	monthly grab	weekly comp. biweekly grab
Particulate P	1995-1997 1998-1999	biweekly grab none	monthly grab none	monthly grab none	biweekly grab none
Dissolved Organic P	1995-1997 1998-1999	biweekly grab none	monthly grab none	monthly grab none	biweekly grab none
Soluble Reactive P	1995-1999	biweekly grab	monthly grab	monthly grab	biweekly grab
Total Dissolved P	1995-1999	biweekly grab	monthly grab	monthly grab	biweekly grab
Calcium	1995-1999	biweekly grab	monthly grab	monthly grab	biweekly grab

Figure 34 depicts a time history of Cell 4 influent and effluent TP concentrations from weekly composite samples. For the first two years of operation, effluent concentrations were dynamic

and exhibited seasonal (winter) increases in effluent concentration. However since mid-1997, effluent concentrations have been stable and have averaged 15 µg/L.

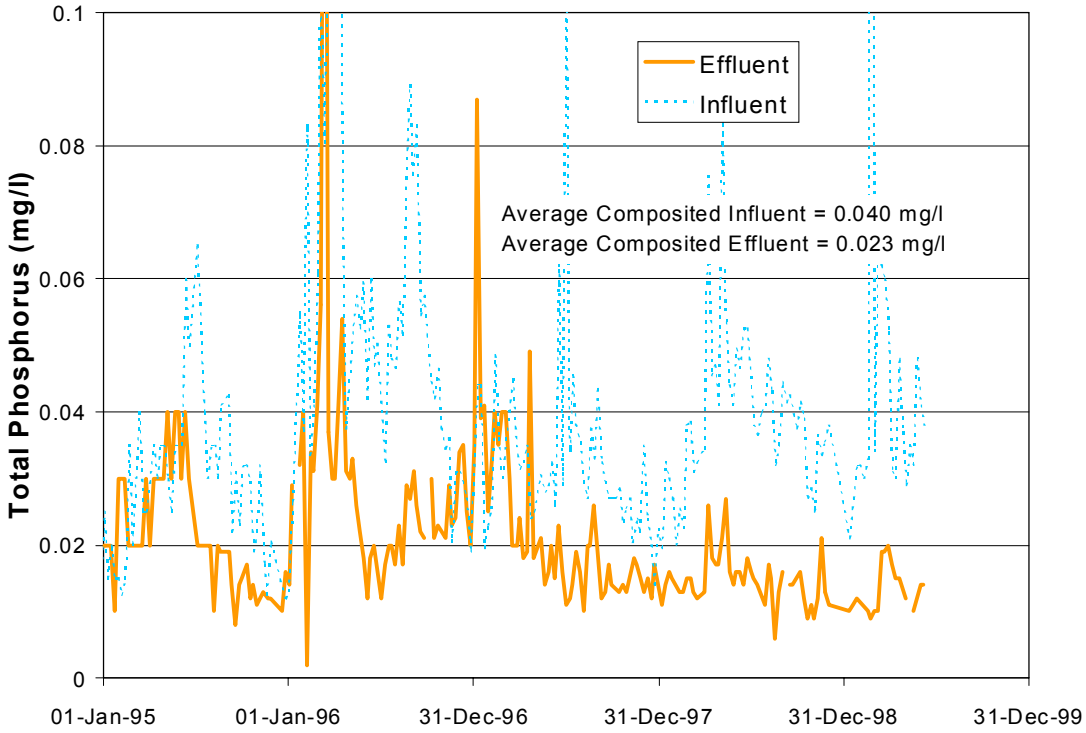

Figure 34. Cell 4 influent and effluent TP concentrations from samples taken three times daily and composited weekly.

Figure 35 shows Cell 4 TP data (weekly composite) plotted on a Julian calendar basis. The heavy line shows average TP performance, which was calculated by each calendar week in the 5.5-year data set. Average effluent TP indicates a seasonal increase in TP export occurring in winter and early spring. This tendency, however, is primarily an artifact of the first three years' performance and does not represent the higher P removals that occurred in recent years (Figure 34). The data suggests full-scale SAV systems may have a several-year start-up period before optimal performance is realized.

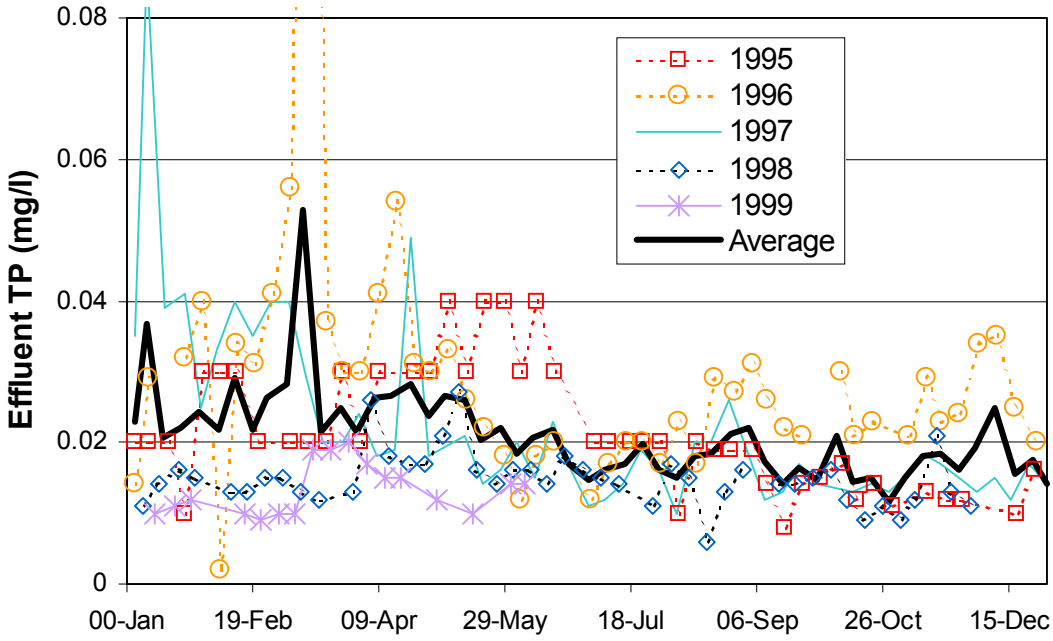

Figure 35. Cell 4 effluent TP concentrations on an annual basis**.**

Figure 36 shows calculated Cell 4 mass removal rates plotted on a Julian basis. Mass removal rates were calculated daily with the following equation:

$$Mass\ \ removal\ rate\ (g/m^2/day) = Inflow*[TP]_{\inf\ luent} + Rain*[TP]_{rain} - Outflow*[TP]_{effluent} - Seepage*[TP]_{effluent}$$

Daily inflow, rain, outflow, and seepage estimates (units of m^3/day) were available from Cell 4 water budget data. Daily influent and effluent TP concentrations were estimated from weekly composite TP data by assuming that the weekly composite value also applied to all non-sampled days. Total P concentrations in rain were assumed to be 16 µg/L for all rain events, and TP concentration in seepage loss was assumed equal to the effluent concentration. The TP concentration in rainfall was estimated from 4.8 year totals of ENR rainfall volume and mass of TP in rainfall, as reported in the District's Everglades' Consolidated Report 2000. Daily mass removals were multiplied by 365 for estimates of annual removal rates, and averaged with a 30-day rolling average (15 days before, 15 days after) to smooth data and retention time effects. The heavy line in Figure 36 indicates the average annual Cell 4 mass removal performance. Historically, TP mass removal has been most effective in summer months.

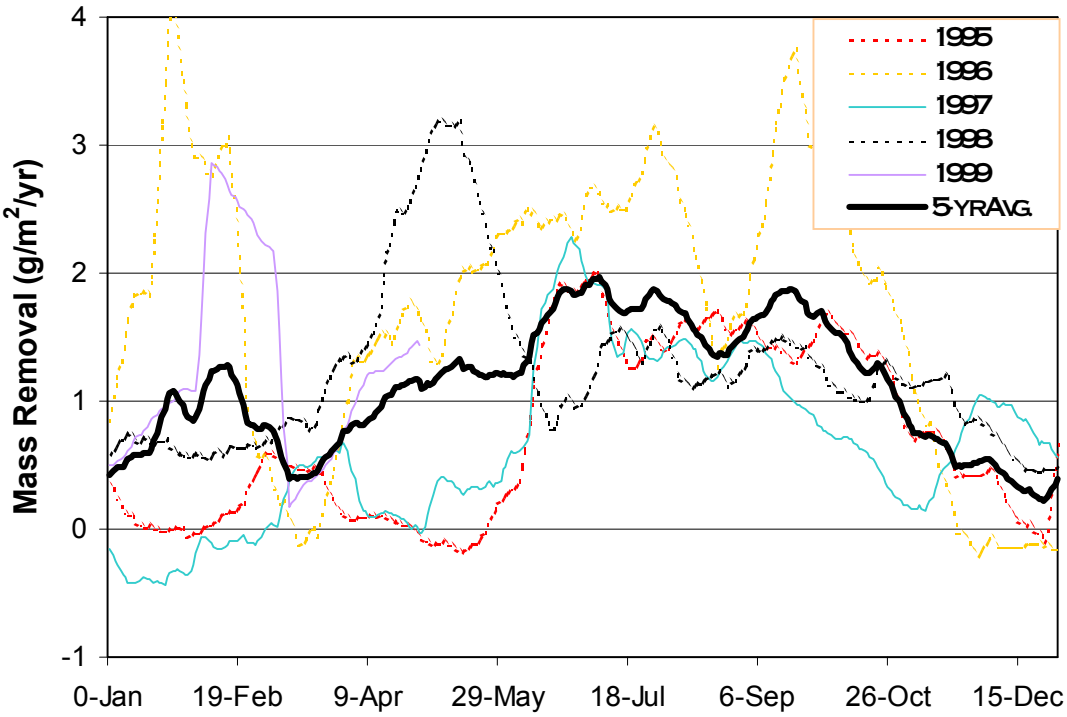

Figure 36. Cell 4 TP mass removal rates on an annual basis. Data were smoothed with a 30-day rolling average.

Figure 37 shows Cell 4 settling rate, k, plotted on a Julian basis. Settling rates were calculated daily with the following equation:

$$Settling\ Rate, k\ (\mathrm{m/yr}) = -\mathrm{Inflow}(\mathrm{m/yr}) * \ln\frac{[\mathrm{TP}]\mathrm{effluent}(\mathrm{g/m^3})}{[\mathrm{TP}]\mathrm{influent}(\mathrm{g/m^3})}$$

Daily settling rates were multiplied by 365 and averaged with a 30-day rolling average for rolling estimates of annual settling rate. Historically, summer months have had the highest TP settling rates. For 1995, 1996, and 1997, negative settling rates evident during winter months correspond to periods when effluent TP concentrations exceeded influent concentrations (Figure 34). Since mid-1997, there have been no other incidents of negative settling rates, suggesting that these may have been related to "start-up" phenomena.

Figure 38 shows TP removal efficiency for Cell 4. Removal efficiency was calculated daily with the following equation:

$$Removal\ Efficiency\ (\%) = \frac{Mass\ TP\ Removed\ (\mathrm{g/m^2/yr})}{Mass\ TP\ Loaded\ (\mathrm{g/m^2/yr})} * 100$$

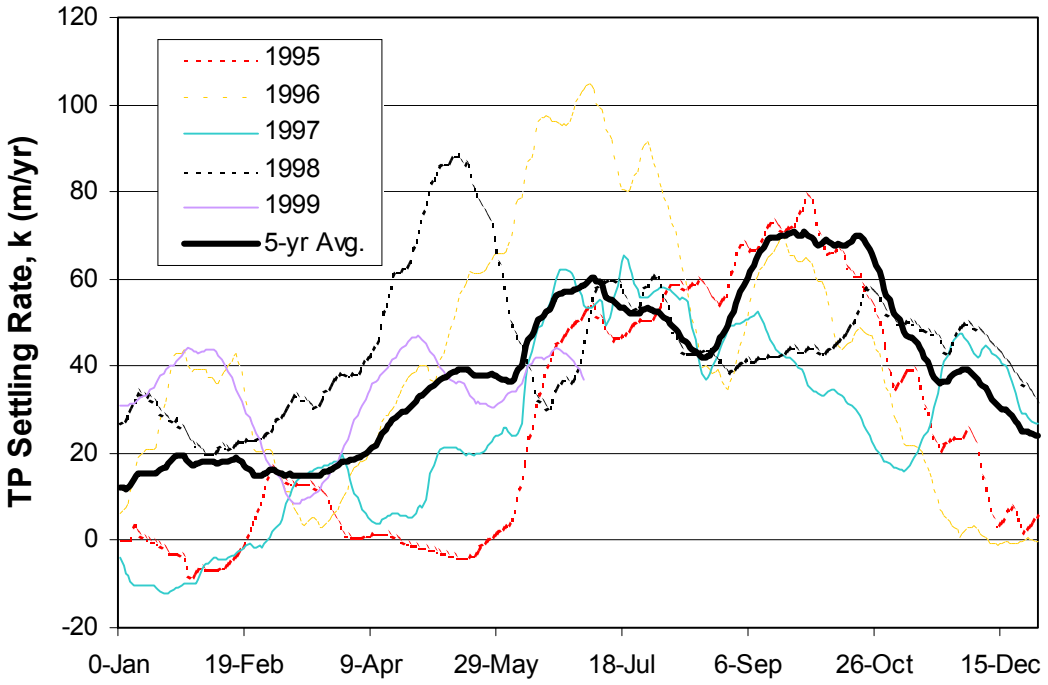

Figure 37. Cell 4 TP settling rate, k, on an annual basis, smoothed with a 30-day rolling average.

where the mass of TP loaded is the product of daily inflow and TP concentration. As with mass removal and settling rate, removal efficiency was greatest in summer months.

Table 9 summarizes annual Cell 4 performance since 1995 based on weekly composite TP data. Note that since 1996, annual average TP concentrations in Cell 4 effluent have consistently declined. Effluent concentrations in the first half of 1999 averaged 13 µg/L, while mass removal, settling rate, and removal efficiency were all above historic averages.

Figure 39 and Figure 40 compare total P concentrations of weekly composite samples (collected 3x/day, 7 days/week) with bi-weekly grab samples for Cell 4 influents and effluents, respectively. We will be using the historic bi-weekly grab data (SRP, DOP, PP, Ca) to begin establishing input/output files for dynamic simulation modeling since we intend for the model to capture phosphorus speciation processes. The comparison between Figure 39 and Figure 40

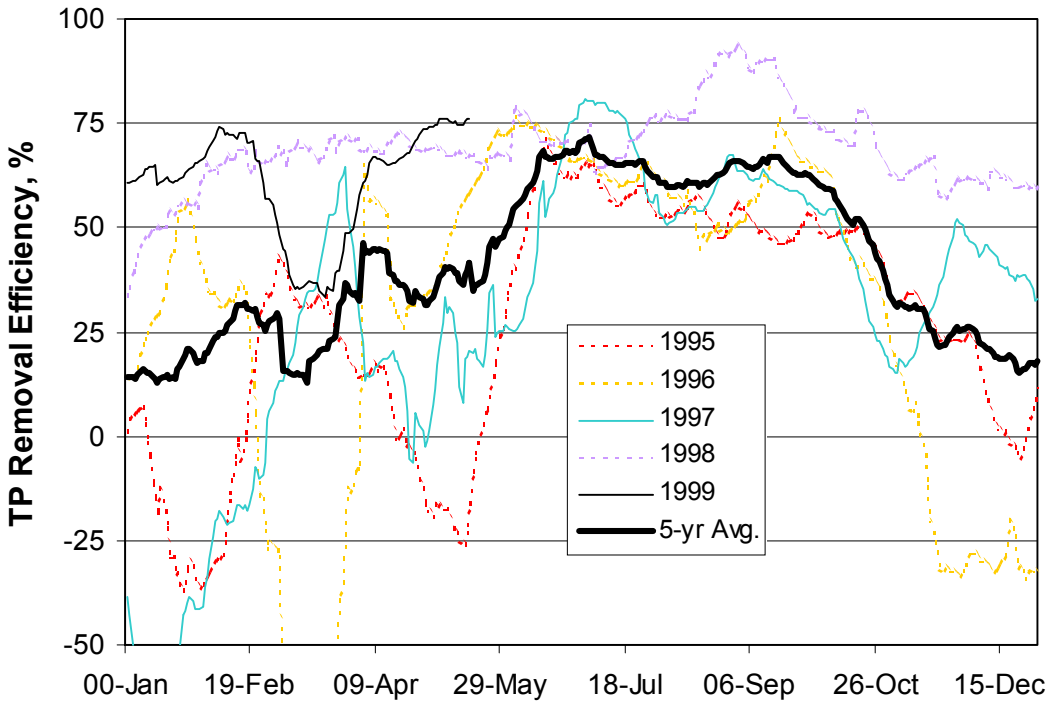

Figure 38. TP removal efficiency in Cell 4 on an annual basis.

Table 9. Summary of Cell 4 TP performance

Year	Effluent TP Concentration (µg/L)	Mass Removal Rates ($g/m^2/yr$)	TP Settling Rate, k (m/yr)	Removal Efficiency (%)
1995	21	0.7	28	26
1996	29	1.7	49	31
1997	21	0.7	26	30
1998	14	1.2	44	70
1999 (1^{st}-half)	12	1.2	43	65
Average	21	1.1	38	43

indicates that over the five-year monitoring period, bi-weekly grab samples produced similar trends as did weekly composites. Average TP concentrations from composite and grab samples also compare favorably. These comparisons suggest that the District's historic bi-weekly grab data adequately capture long-term Cell 4 dynamics and will be adequate for simulation model input/output files.

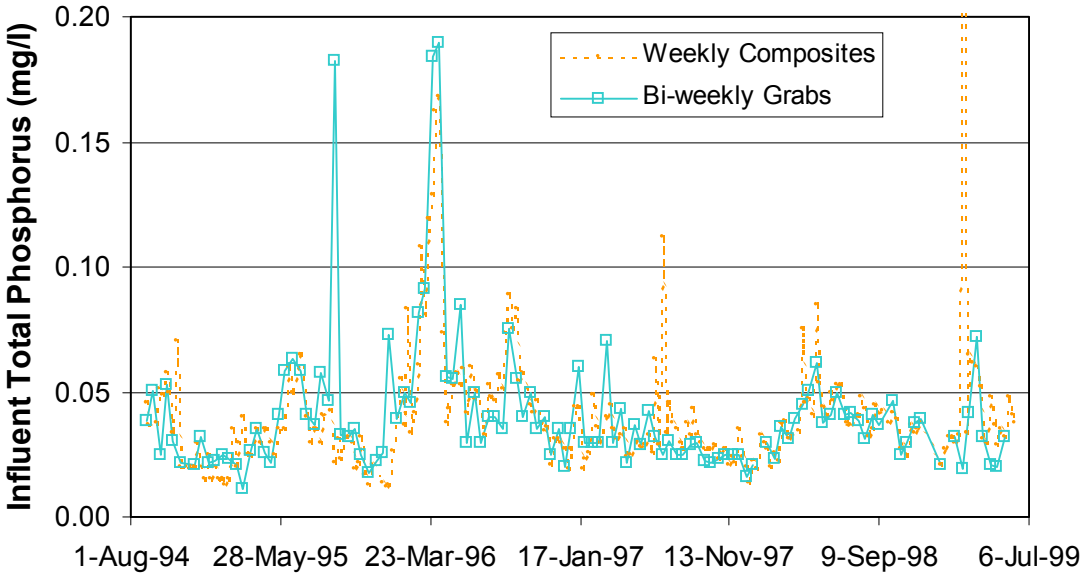

Figure 39. Comparison of bi-weekly grab and weekly composite TP samples for Cell 4 influent.

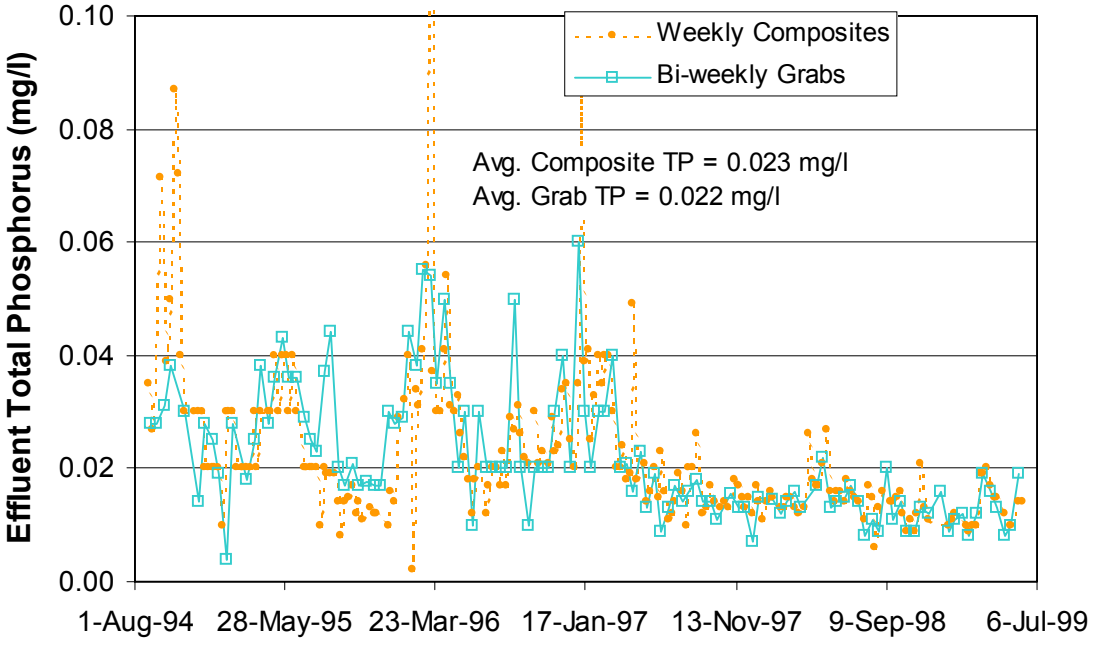

Figure 40. Comparison of bi-weekly grab and weekly composite TP samples for Cell 4 effluent.

Figure 41 depicts annual phosphorus concentrations along a horizontal gradient within Cell 4. The horizontal gradient is represented by data collected at four sampling locations: influent culverts (G254), one-third distance along the cell length (ENR401), two-thirds distance along the cell length (ENR402), and effluent culverts (G256). The plotted data in Figure 41 are annual averages of bi-weekly grab sample data for influent and effluent stations, and averages of monthly grab sample data for the two internal stations. As noted above, effluent TP from Cell 4 has steadily decreased since 1996. For the first half of 1999, the bi-weekly grab data indicate an average TP concentration in Cell 4 effluent of 12 µg/L, which compares favorably with the 13 µg/L reported from weekly composite data. In general, PP and SRP fractions are noticeably reduced with Cell 4 treatment. However, DOP fractions throughout Cell 4 do not decrease as substantially as PP and SRP fractions.

The average annual data for TP, SRP, pH, and calcium along the same spatial gradient are provided in Figure 42. The TP data indicate that after the 1995/1996 start-up years, the TP concentration drops most substantially within the first two-thirds of Cell 4. Note that there is little, if any, evidence of additional P removal in the lower one-third of Cell 4 for any year.

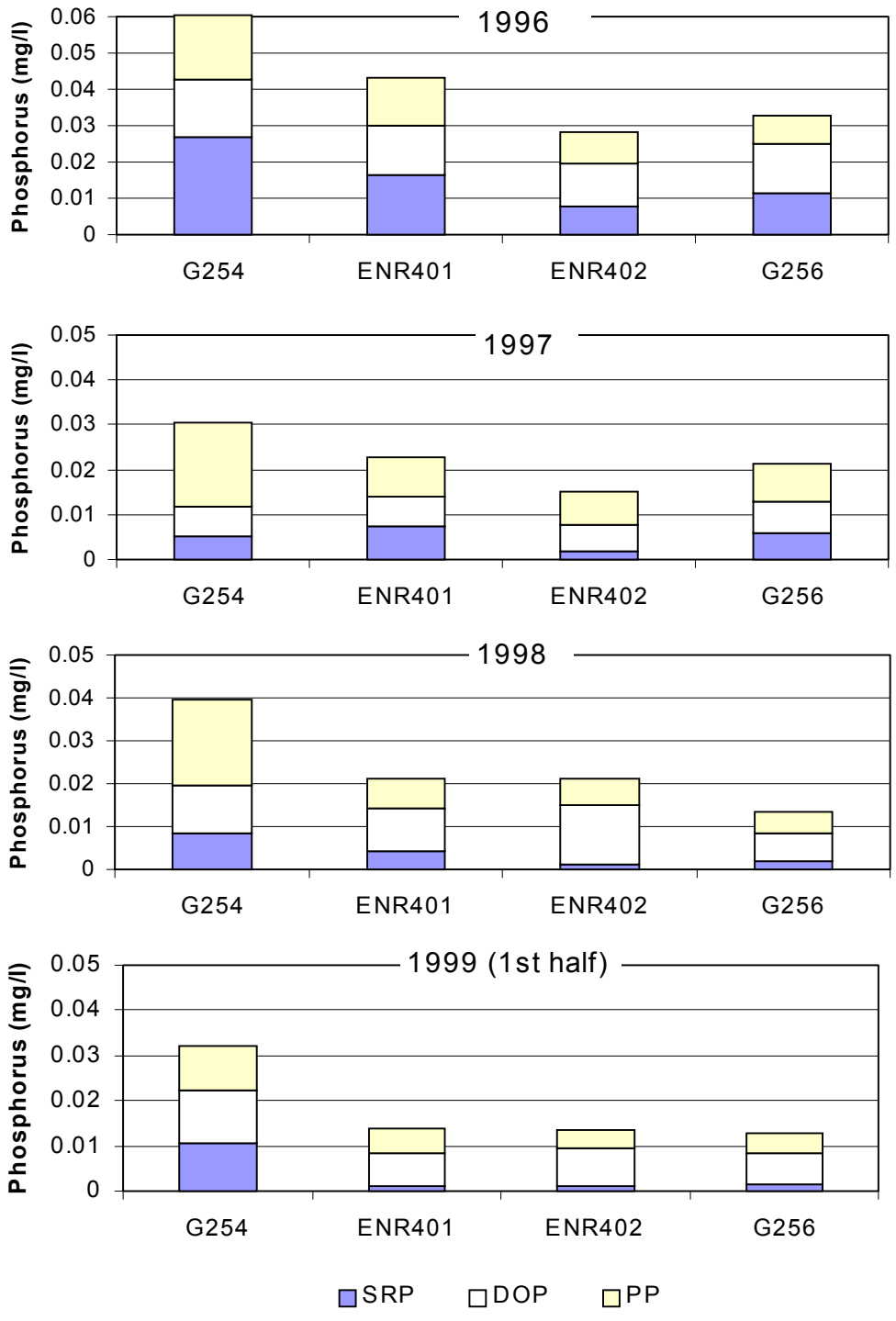

Figure 41. Annual concentrations of phosphorus species in Cell 4 based on grab sample data. Influent is at G254. ENR401 and ENR402 are internal sampling locations approximately one-third and two-thirds distance from inflow, respectively. Effluent is at G256.

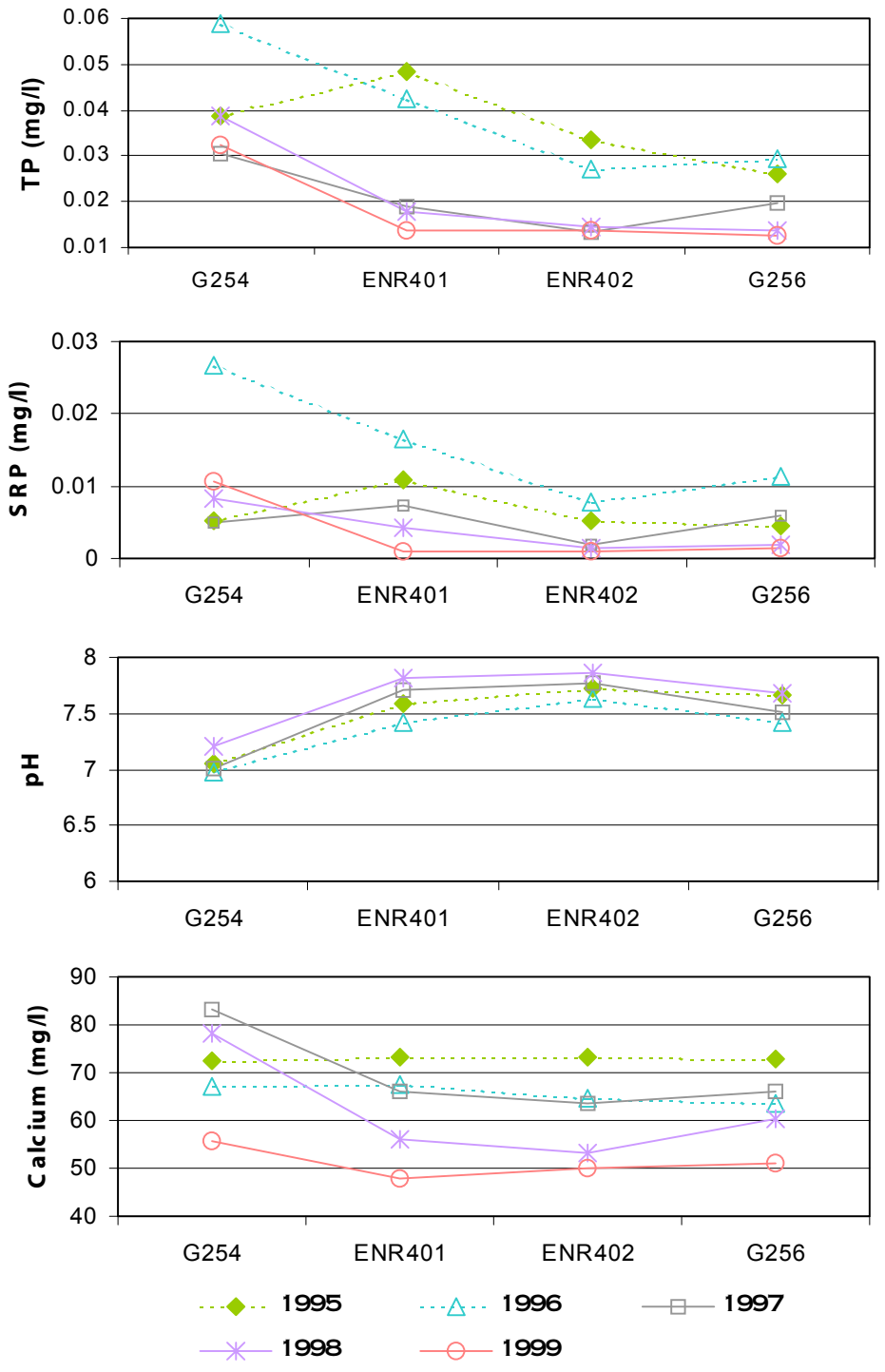

Figure 42. Spatial gradients of TP, SRP, pH, and Ca in Cell 4.

Forecast Model Development

Introduction

Over the course of the Phase II project, we are developing a process-based dynamic simulation model for SAV treatment systems. Developing the model provides a means for integrating data and concepts generated in the many multi-scale experiments in the project. Our goal is a simple, yet highly useful, representation of processes and characteristics unique to SAV systems. The calibrated model will be used in addressing three research questions: defining the ultimate P removal potential (C*) in SAV systems, predicting system response to disturbance, and predicting long-term sustainability of SAV performance.

Input and Calibration Data

During this reporting period, input and calibration files were assembled for the simulation model. The input file was derived from hydrological and water quality data for Cell 4. Because we intend to run simulations using a daily time increment, we therefore constructed input and calibration files with measured and estimated daily influent and effluent data.

As described above, we have prepared an accurate daily water budget from January 1995 through April 1999 for Cell 4. The water budget was based on measured inflow, outflow, and precipitation data and District estimates of seepage and evapotranspiration losses. The Cell 4 water budget provides all necessary hydrologic data required for simulation modeling. Influent water quality data were added to the water budget spreadsheet to provide a complete input file for simulation modeling. As noted above, TP, SRP, DOP, PP, and Ca data were available from bi-weekly grab samples. For the input file, daily influent water quality was estimated by applying measured bi-weekly constituent concentration values to all non-sampled days in the previous two weeks. TP data were also available from weekly composite data, and these data were also included in the simulation input file.

The model will be calibrated to historical Cell 4 effluent data. The calibration procedure will select model coefficients in order to meet two criteria:

1. The mean simulated effluent concentration will equal the mean measured effluent concentration over the simulation duration.

2. The following error function between simulated and measured effluent concentrations will be minimized:

$$Average\ Daily\ Error = \sqrt{\frac{\sum_{n=1}^{\#\ days}(simulated\ concentration - actual\ concentration)^2}{\#\ days}}$$

To calculate the error function on a daily basis, effluent data from bi-weekly grab samples (TP, SRP, DOP, PP, and Ca) were expanded into a daily calibration file using the same extrapolation technique described above.

Model Format and Programming

During this reporting period, programming efforts were initiated for the dynamic simulation model. The simulation model is being written as a Visual BASIC program within an EXCEL input/calibration spreadsheet. The Q-Basic program reads the input file from the spreadsheet, performs modeling calculations, and returns columns of simulation output to the spreadsheet. The EXCEL spreadsheet is used for all post-processing, including error function calculation and data smoothing as well as presentation charts and graphs.

The model's mathematics express dynamic relationships between model variables with differential equations. The differential equations are programmed in Q-Basic using finite difference equations. To insure calculation stability under dynamic loading, the Q-Basic program has the capacity to divide each day's calculations into user-specified increments. The more calculation increments per day, the smaller the potential for calculation error, but at the price of longer calculation times. As model complexity increases, it may be necessary to run the program using 10-100 calculation intervals per day to avoid error accumulations.

Simulation Modeling

During this reporting period two models were programmed and calibrated. The first model is a dynamic first-order TP removal model based on the complete water budget. A schematic diagram in Figure 43 illustrates the model configuration. The rectangular border in Figure 43

represents the Cell 4 system. The water budget components are shown around the periphery of the cell. Water enters the system with rain and influent flows and leaves the system in evaporation, effluent flow, and seepage. Total phosphorus is stored in the water column and in sediment; we have not yet, however, modeled biomass storage. The model assumes that Cell 4 acts as a continuously stirred tank reactor (CSTR) and that water concentration throughout the cell is homogeneous. TP is carried into the system in rain and influent flows and is carried out of the system in effluent and seepage flows. In accordance with the CSTR assumption, TP in effluent and seepage flows are the same concentration as is in the water column. In addition to effluent and seepage flows, the model assumes that TP is removed from the water column and stored in inactive sediment at a rate proportional to the daily TP concentration in the CSTR (i.e., 1st order removal).

The equation that defined the behavior of the TP water column storage in the model was as follows:

$$\frac{d(TP)}{dt} = Influent * [TP]_{In} + Rain * [TP]_{rain} - Effluent * [TP]_{CSTR} - Seepage * [TP]_{CSTR} - K * [TP]_{CSTR}$$

where: d(TP)/dt = daily change in stored TP mass on a real basis, (g/m^2/day)

$[TP]_{in}$ = influent TP concentration, (g/m^3)

$[TP]_{rain}$ = TP concentration in rain, (0.016 g/m^3)

$[TP]_{CSTR}$ = TP concentration in water column, (g/m^3)

K = coefficient of first-order removal, (m/day)

Influent, Rain, Effluent, Seepage = daily flows, (m/day)

The TP concentration in rainfall (0.016 g/m^3) was estimated from 4.8 year totals of ENR rainfall volume and mass of TP in rainfall, as reported in the District's Everglades' Consolidated Report 2000.

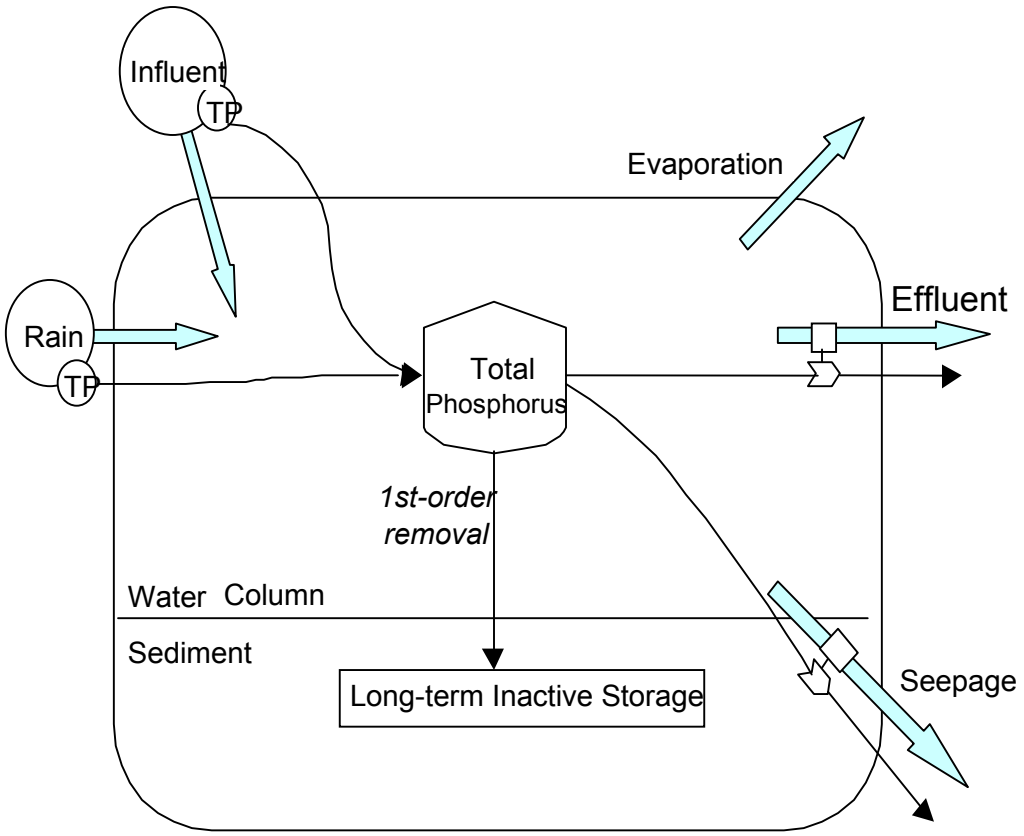

Figure 43. Model diagram for simulation of first-order TP removal in Cell 4 based on daily water balance and measured TP concentration data.

Results of the calibrated first-order simulation model are shown in Figure 44. Figure 44(a) compares the simulated TP concentration to measured grab sample data. The simulated TP data were smoothed using a 14-day rolling average (7 days before, 7 days after). The calibrated removal coefficient, K, was equal to 37 m/year. The average simulated effluent TP concentration was 21 µg/L, which equaled the average TP concentration from bi-weekly grab data. The average daily error in simulated TP was 13.6 µg/L. Figure 44(b) shows a partitioning of average TP flows over the 4.3-year simulation period. Rain accounts for approximately 5% of TP loading to the Cell 4. The model suggests that Cell 4 removes approximately 38% of entering TP to inactive sediment, while 56% leaves in effluent and 6% leaves in seepage.

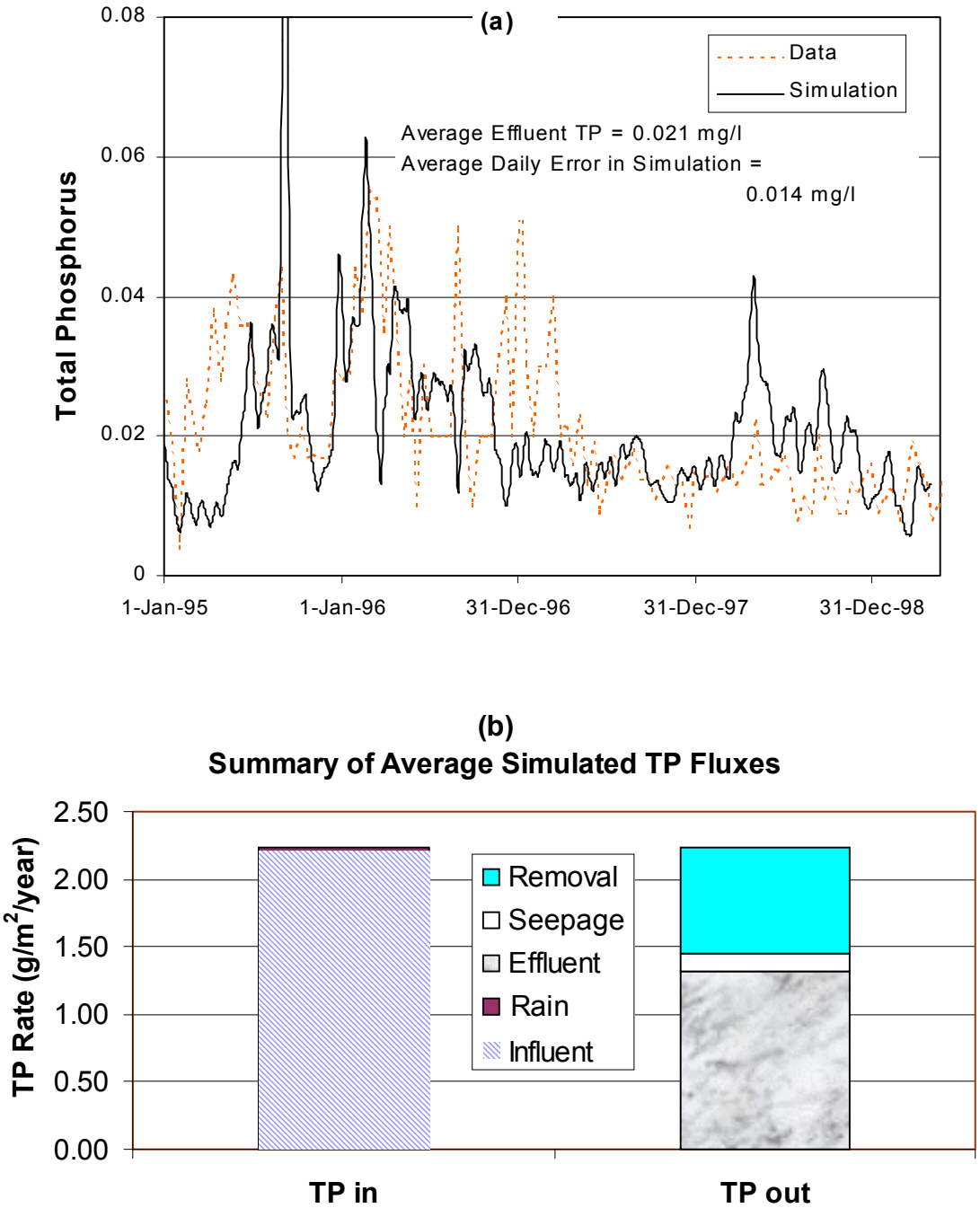

Figure 44. Simulated Cell 4 effluent TP concentrations compared to TP data collected with weekly grab samples (a) and partition of TP flows averaged over simulation period (b). Model is based on first-order removal of total phosphorus. Simulated data is smoothed with 14-day rolling average.

A second model was also developed and calibrated. This model divided TP into two independent storages, SRP and PP+DOP. A schematic diagram illustrating the model is shown in Figure 45. Each of the two storages has a first-order removal coefficient; total phosphorus removal is the sum of SRP and PP+DOP removals. Calibration was carried out in two steps. First, K_{SRP} was chosen to calibrate simulated SRP to measured SRP data. Second, K_{PP+DOP} was chosen to calibrate the sum of simulated PP+DOP to measured sum of PP and DOP data. Figure 46(a) shows the simulated TP time history and Figure 46(b) shows the average partitioning of phosphorus fluxes over the 4.3-year simulation. The calibrated SRP removal coefficient, K_{SRP}, was 40 m/yr, while K_{PP+DOP} was 22 m/yr.

The two models produced similar time histories of simulated TP (Figure 46a and Figure 44a). The average error in both simulations was large compared to the average effluent concentration. The two parameter model did not improve simulation accuracy over the single parameter model; in fact, net accuracy decreased with the two parameter model. Table 10 summarizes key results from the two first-order simulation models. The simulation results suggest that the PP+DOP fraction is less efficiently removed than the SRP fraction from Cell 4 waters; the removal constant for combined PP+DOP fraction was only 55% of the SRP removal constant.

Both of these models do a poor job of simulating measured effluent TP concentrations (Figure 44a and Figure 46a). Simple first-order removal models are very limited in that phosphorus is only removed in direct proportion to water-column concentrations. First-order removal models do not take into account the actual processes occurring in a wetland that leads to P removal, and these processes may or may not act proportionately to water column concentration. Our future modeling efforts will focus on simulating internal biogeochemical processes in SAV systems, with the intent of improving model accuracy and utility.

Table 10. Summary of Simulation Modeling

Model	Calibration Constants	Average Error
1^{st} – order: TP	K_{TP} = 37 m/year	13.6 µg/L
1^{st} – order: SRP	K_{SRP} = 40 m/year	7.0 µg/L
1^{st} – order: PP+DOP	K_{PP+DOP} = 22 m/year	13.0 µg/L

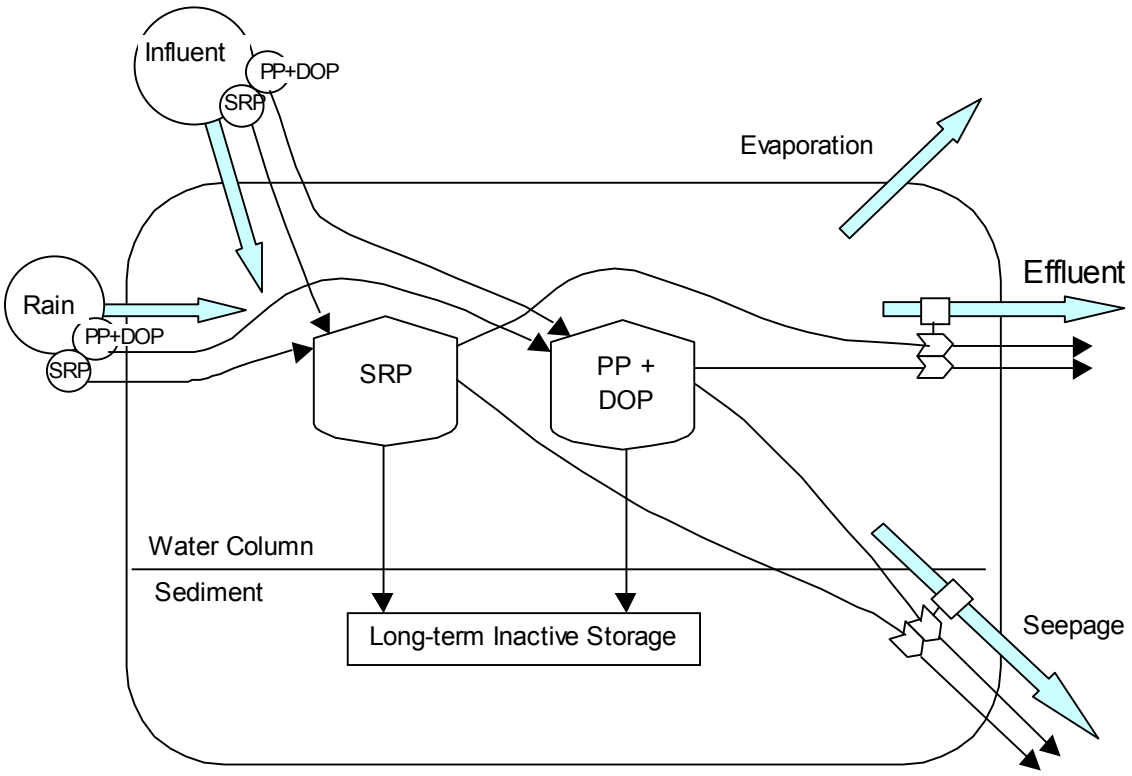

Figure 45. Modeling diagram for simulation of first-order removal of SRP and PP+DOP fractions.

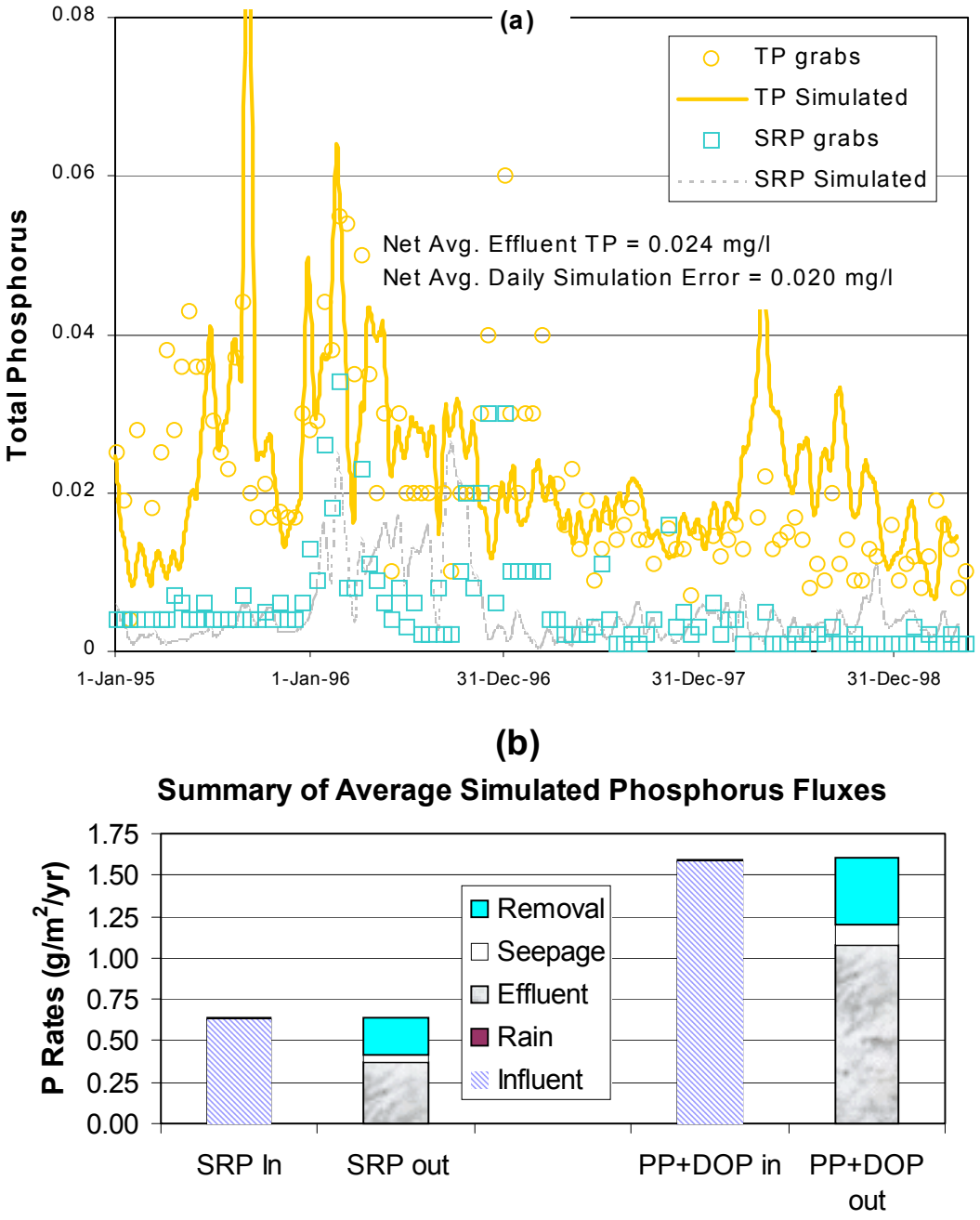

Figure 46. Simulated Cell 4 effluent TP concentrations compared to TP data collected with bi-weekly grab samples (a) and partition of TP flows averaged over simulation period (b). Model is based in parallel path first-order removal for SRP and PP+DOP species. Simulated data are smoothed with 14-day rolling average.

Task 9 References

Redfield, G. Ed. 2000. Everglades Consolidated Report, South Florida Water Management District and Florida Department of Environmental Protection.

Task 10. Investigations of Techniques for Inoculating SAV into STA Cells

STA-1W Cell 5 was flooded in late spring 1999, but has continued to exhibit high water column levels of both phosphorus and color. The previously disturbed (farmed) organic soils are thought to be the source of the high water column constituent concentrations. As part of our work scope, we are investigating the colonization rate of SAV into Cell 5, inoculation techniques for SAV that might be suitable for large-scale wetland applications, and the use of a chemical amendment (lime) to reduce water column TP and color concentrations.

Small-scale jar tests have demonstrated that lime can lower color and TP levels of Cell 5 waters. However, it is unknown how effective general broadcasting of lime into the large wetland cell will be, since there would be little mixing energy compared to that provided in jar tests, and because the organic soils may continue to act as a source of P and TOC.

To test the effectiveness of lime additions, we deployed *in situ* chambers (46 cm diameter transparent fiberglass cylinders) to isolate small portions of the Cell 5 sediments and water column. Six columns were deployed, with duplicate columns for each of these treatments: control, low lime dose, and high lime dose. We selected 66 mg/L and 198 mg/L as $Ca(OH)_2$ for the low and high dosages, respectively. On November 9, 1999 the lime was added to the water surface in four of the six columns, with no mixing provided. We discovered contamination (a large, dead fish) in one of the columns on the first sampling date, so only one control column was monitored during the experiment. In addition to that Column Control, surface water outside the columns (i.e., an Ambient Control) was analyzed to discern if any "enclosure" effects had occurred.

Following lime addition, the water column was sampled at 0 and 4 hr, and 1, 3, 7, 14, 21, 28 and 42 days, for temperature, pH, SRP, TP, total Ca, alkalinity, and color (apparent and true).

After 24 hours, the SRP concentrations in the two sets of controls (water outside the enclosures [Ambient Control] and water inside the enclosure [Column Control]) diverged, as did the total P

concentrations (Figure 47). The two types of controls were within close agreement with respect to true and apparent color, total calcium, and total alkalinity throughout most of the study period (Figure 47).

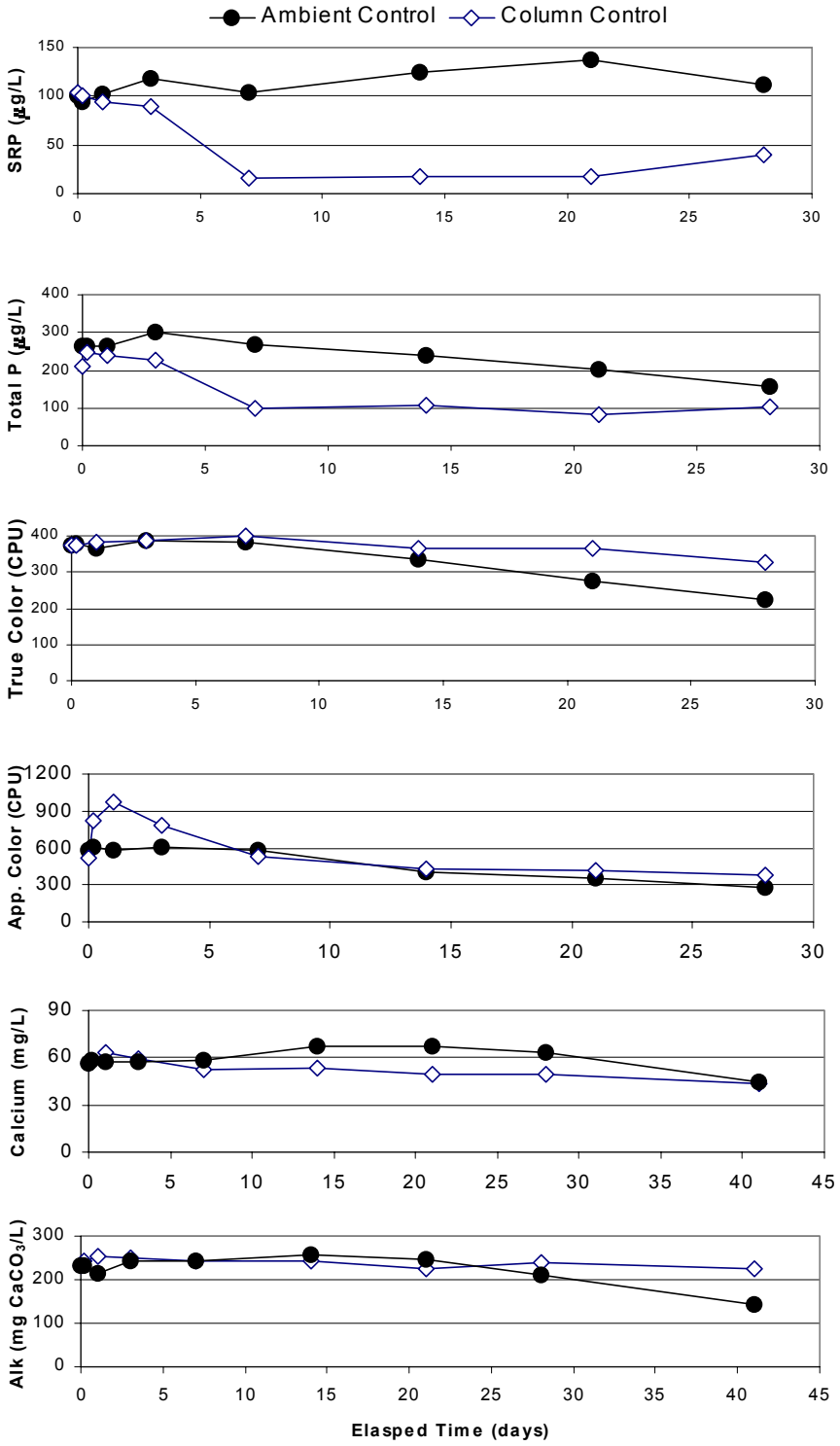

Figure 47. Concentrations of SRP, total P, true and apparent color, alkalinity and calcium for Cell 5 water outside (Ambient Control) and inside (Column Control) *in situ* columns during November 9 – December 7, 1999.

Compared to the Column Control, both lime dosages provided lower concentrations of SRP and total P in Cell 5 surface water for the first three days. Both TP and SRP concentrations converged on the seventh day (Figure 48). For both lime dosages, SRP concentrations decreased from an average of 141 to 4 µg/L within the first 4 hours. By the third day, SRP concentrations had increased to 13 µg/L in both sets of dosed columns, which was still considerably lower than the 89 µg/L concentration in the Column Control. Total P concentrations, on the other hand, decreased to approximately half the Column Control values within the first three days (Figure 48). The differences between dosing treatments (66 vs. 198 mg $Ca(OH)_2$) in P removal were minimal.

Apparent color (unfiltered) concentrations were initially elevated in the pair of high dosage columns because of the increased turbidity from calcium carbonate precipitation, but the effect was short-lived (Figure 48). After the first day, the changes in apparent color concentrations within the Column Control and the lime-amended columns tracked each other closely for 28 days.

True color is a better measure for characterizing the removal of dissolved organic matter (DOM) than is apparent color since turbidity interference is removed by filtering the sample. Most removal of the DOM occurred immediately at the onset of the high dosage lime amendment where the color concentration was nearly reduced by half within the first day (Figure 48). Over the 28-day measurement period, more of the DOM was removed in the higher dosed columns than the moderately dosed columns.

Relative to the Column Control, total calcium and alkalinity concentrations declined inside the enclosures that received the lime (Figure 48); lower concentrations were observed up to 14 days for calcium and 28 days for alkalinity. Since the decreases in calcium and alkalinity concentrations during the first two weeks were due to the precipitation of calcium carbonate, the higher removals in the high dosage columns were expected (Figure 48).

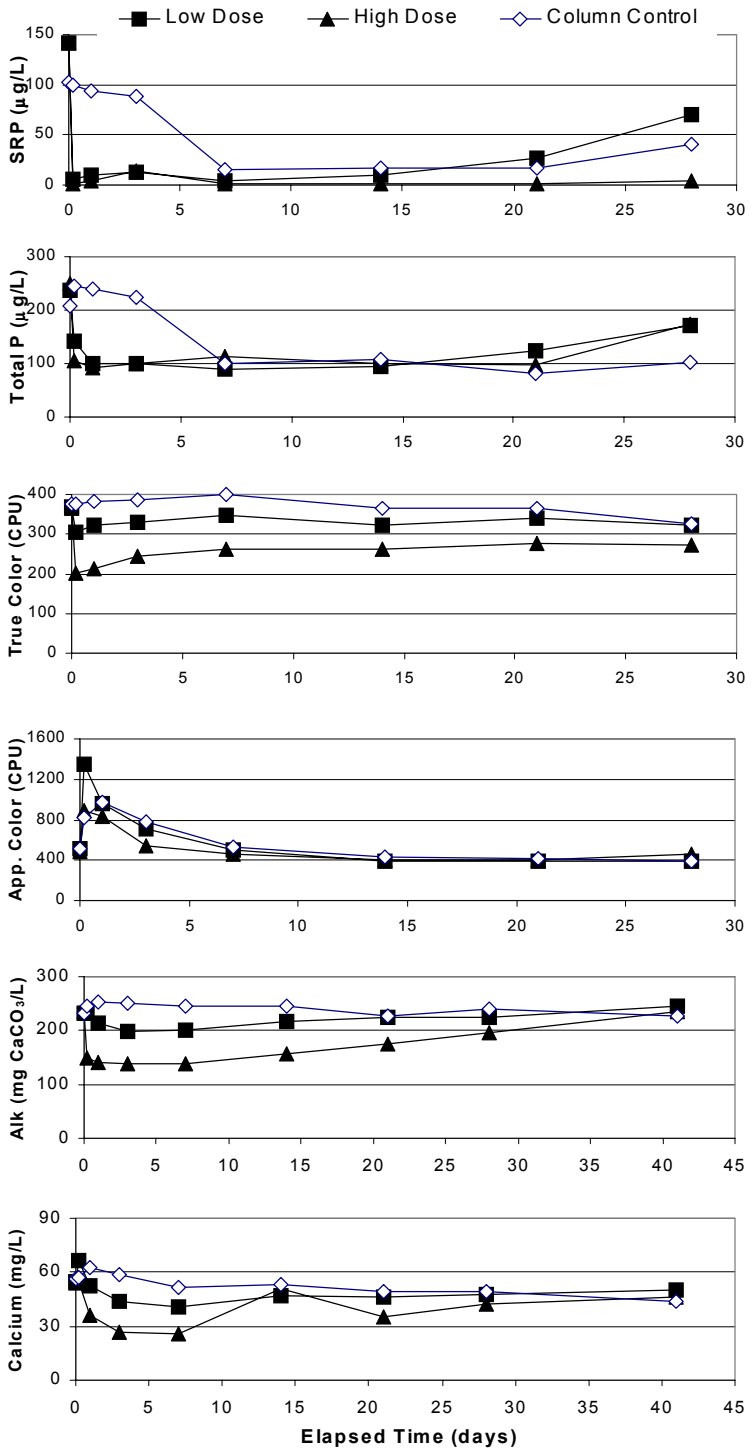

Figure 48. Concentrations of SRP, total P, true and apparent color, alkalinity and calcium for Cell 5 water contained within *in situ* columns receiving Low Dose (66 mg/L; duplicate columns) and High Dose (198 mg/L; duplicate columns) lime additions (as $Ca(OH)_2$). The Column Control was not dosed.

The longevity of the SRP removal appears at first to last 28 days in the High Dose columns and 21 days in the low-dosed columns (Figure 48). However, the single untreated Column Control also removed SRP nearly as efficiently beginning on the seventh day, indicating "enclosure" effects may have influenced the SRP removal from that day forward. Besides the difficulty of determining the extent of "enclosure" effects during prolonged incubation periods (weeks), there is also the issue of larger, field-scale effects that are not represented within an enclosure. For example, water and sediment turbulence was dampened considerably within the enclosures compared to the external wetland waters and sediments. If lime was applied to all of Cell 5, wind-generated turbulence could either prolong (by resuspending the calcite floc layer) or foreshorten (by dispersing and diluting the sediment floc layer) the period of effective P removal.